

Survey report

MS Eros, MS Kings Bay MS Vendla 14.-26.02.2020



Distribution and abundance of Norwegian spring-spawning herring during the spawning season in 2020

By Are Salthaug, Erling Kåre Stenevik, Sindre Vatnehol, Valantine Anthonypillai, Egil Ona and Aril Slotte

Institute of Marine Research (IMR), P. O. Box 1870 Nordnes, N-5817 Bergen, Norway

Summary

During the period 14-26th of February 2020 the spawning grounds of Norwegian spring-spawning herring from Møre (62°20'N) to Nordvestbanken (70°40'N) were covered acoustically by the commercial vessels MS *Eros*, MS *Kings Bay* and MS *Vendla*. The survey was carried out under challenging weather conditions, however, the collected acoustic and biological data are considered to be of good quality. The estimated biomass was around 24 % lower and the estimated total number was about 10 % lower this year than in the 2019 survey. The uncertainty of the estimate in 2020 was estimated to be higher compared with 2019. The surveyed population was dominated by the 2013 and 2016 year classes. The 2016 year class is estimated to be around three times more abundant than the 2013 year class was as 4 year olds in 2017 (in this survey). The spatial distribution of the spawning stock was similar to earlier years; close to the coast south of Træna and on the slope around the banks outside Lofoten and Vesterålen, with the youngest and smallest herring in the north and older and larger herring in the south. The estimates of relative abundance from the survey in 2020 are recommended to be used in this year's ICES stock assessment of Norwegian spring-spawning herring.

Survey participants 14-26.02.2019:MS Eros

Erling Kåre Stenevik	Survey leader
Lage Drivenes	Instrument/Acoustics
Guosong Zhang	Instrument /Acoustics
Inger Henriksen	Biology
Jostein Røttingen	Biology
Egil Ona	Head of acoustics

MS Kings Bay

Sindre Vatnehol	Survey leader
Reidar Johannesen	Instrument/Acoustics
Sture Vatnehol	Instrument/Acoustics
Adam Custer	Biology
Ørjan Sørensen	Biology

MS Vendla

Are Salthaug	Survey coordinator
Benjamin Marum	Instrument/Acoustics
Magnar Polden	Instrument/Acoustics
Valantine Anthonypillai	Biology
Justine Diaz	Biology

Introduction

Acoustic surveys on Norwegian spring-spawning herring during the spawning season has been carried out regularly since 1988, with some breaks (in 1992-1993, 1997, 2001-2004 and 2009-2014). In 2015 the survey was initiated again partly based on the feedback from fishermen and fishermen's organizations that IMR should conduct more surveys on this commercially important stock. Since then this has continued with a survey design using three commercial vessels, and IMR has contracted the same vessels to run this survey during the period 2017-2020. The ICES WKPELA benchmark in 2016 decided to use the data from this time series as input to the stock assessment, together with the ecosystem survey in the Norwegian Sea in May and catch data, meaning that the results of the survey have significant influence on ICES catch advice.

Hence, the objective of the NSS spawning survey 2020 was to continue the relative abundance estimates for use in the ICES WGWIDE stock assessment, more specifically to estimate indices of abundance and biomass at age during the period of spawning migration from wintering areas

at/off the northern Norwegian coast and in the Norwegian Sea towards the coastal spawning ground further south. Finally, it was also a purpose that the results of the survey should be compared with recent surveys with comparable effort and design during 2015-2019.

Material and methods

Survey design

During the period 14-26th of February 2020 (same period as in 2017-2019) the spawning grounds from Møre (62°20'N) to Troms (70°40'N) were covered acoustically by the commercial fishing vessels *MS Eros*, *MS Kings Bay* and *MS Vendla*.

The survey was planned based on information from the previous spawning cruises and the distribution of the herring fishery during the autumn 2019 up to the survey start February 14 2020 (Figure 1). The fishery prior to the survey start in 2020 indicated that the herring wintering in the Norwegian Sea were entering the coast in the Træna deep south of Røst and following the eastern shelf edge 200 m depth southwards from Træna as also observed in 2016-2019. This information also suggested that smaller and younger herring recruiting to the spawning stock initiated their spawning migration from wintering grounds further north of 70°N west of Tromsøflaket and in the Kvænangen fjord area, which was the basis for the planned survey coverage this far north. As seen from Figure 1, the fishery had already started at Buagrunden (63°N) at the onset of survey in 2020.

The survey design followed a standard stratified design (Jolly and Hampton 1990), where the survey area was stratified before the survey start according to the expected density and age structures of herring (Figure 2). With exception of stratum 13, all strata this year were covered with a zigzag design instead of parallel transects. The introduction of a zigzag design started in 2018. Compared with parallel transects, zigzag design is more efficient since a higher proportion of the sailed distance is used for coverage (Harbitz 2019). In 2015-2017, a significant part of the survey time was used as transport between transects, whereas in 2018-2020 insignificant time was used on transport. Each straight line in the zigzag design were considered as transects and primary sampling units (Simmonds and MacLennan 2008), with fairly uniform coverage of strata and a random starting position in the start of each stratum. In order to investigate potential herring aggregations west of Buagrunden (it has previously been stated by

some fishermen that herring arrives on the Buagrunnen directly from the Norwegian Sea, i.e. from west) two parallel transects were covered extending approximately 80 nautical miles west of Buagrunnen (63°N).

Biological sampling

Trawl sampling was carried out on a regular basis during the survey to confirm the acoustic observations and to be able to give estimates of abundance for different size and age groups. All three vessels used commercial herring trawls with small meshed (20 mm) inner net in the codend, and with a slit (so called “splitt”) close to the codend to avoid too large catches. The positions of the trawl hauls are shown in Figure 3. The following variables of individual herring were analysed for each station with herring catch: Total weight (W) in grams and total length (L_T) in cm (rounded down to the nearest 0.5 cm) of up to 100 individuals per sample. In addition, age from scales, sex, maturity stage, stomach fullness and gonad weight (W_G) in grams were measured in up to 50 individuals per sample. The maturation stages were determined by visual inspection of gonads as recommended by ICES: immature = 1 and 2, early maturing = 3, late maturing = 4, ripe = 5, spawning = 6, spent = 7 and resting/recovering = 8. Data from the subjective evaluation of maturation stages were used to split between immature and mature herring in the estimation of spawning stock biomass (SSB), as well as to demonstrate spatial differences in maturation. The gonadosomatic index ($GSI = \text{gonad weight} / \text{total weight} \times 100$) was also used to demonstrate spatial differences in maturation along the coast.

Environmental sampling

CTD casts (using Seabird 911 systems) were taken by Eros and Vendla, spread out in the survey area (Figure 3).

Echo sounder data

Multifrequency (18, 38, 70, 120, 200 kHz) acoustic data were recorded with a SIMRAD EK 60 echo sounder and echo integrator on board Eros and Vendla, and SIMRAD EK 80 on board Kings Bay. Continuous Wave (CW) pulse, i.e. single frequency, was transmitted from all sounders. All three vessels were calibrated at the tip of the fishing pier in Ålesund prior to the survey according to standard methods (Foote et al., 1987), adjusted for split beam methods as described in Ona (1999) and (Demer et al. 2015). The calibration reports of each vessel are shown in Annex 1. The low frequency sonars were not calibrated. The intention was only to use the sonar data for studies of potential issues with herring in the echo sounder blind zone

close to the surface or avoidance, not for biomass estimations of schools. Hence, a new calibration of the sonars was not considered necessary.

LSSS, Large Scale Survey System (Korneliussen et al., 2006) was applied for the interpretation of the multi-frequency data. The recorded area echo abundance, i.e. the nautical area backscattering coefficient (NASC) (MacLennan et al. 2002), was interpreted and distributed to herring and ‘other’ species at 38 kHz. Various characteristics of the acoustic recordings like frequency response (Korneliussen and Ona 2002) and visual appearance were used to identify herring from other targets.

In 2020 the survey suffered from relatively bad weather condition, like last year. During conditions where the vessels had to survey against strong winds, acoustic registrations on some transects were significantly influenced by air bubble attenuation. This was corrected for during the scrutinization of the data in LSSS, and the problems and methods used to adjust is described in Annex 3 in last year’s cruise report (Slotte et al. 2019). However, only a small fraction of the acoustic values had to be corrected in this year’s survey.

Abundance estimation methods

The acoustic density values were stored by species category in nautical area scattering coefficient (NASC) [$\text{m}^2 \text{n.mi.}^{-2}$] units (MacLennan et al. 2002) in a database with a horizontal resolution of 0.1 nmi and a vertical resolution of 10 m, referenced to the sea surface. To estimate the mean and variance of NASC, we use the methods established by Jolly and Hampton (1990) and implemented in the software StoX (Johnsen et al. 2019). The primary sampling unit is the sum of all elementary NASC samples of herring along the transect multiplied with the resolution distance. The transect (t) has NASC value (s) and distance length L . The average NASC (S) in a stratum (i) is then:

$$\hat{S}_i = \frac{1}{n_i} \cdot \sum_{t=1}^{n_i} w_{it} s_{it} \quad (1)$$

where $w_{it} = L_{it} / \bar{L}_i$ ($t= 1,2,.. n_i$) are the lengths of the n_i sample transects, and

$$\bar{L}_i = \frac{1}{n_i} \sum_{t=1}^{n_i} L_{it} \quad (2)$$

The final mean NASC is given by weighting by stratum area, A ;

$$\hat{S} = \frac{\sum_i A_i \hat{S}_i}{\sum_i A_i} \quad (3)$$

Variance by stratum is estimated as:

$$\hat{V}(\hat{S}_i) = \frac{n}{n_i - 1} \sum_{t=1}^n w_{it}^2 (s_t - \bar{s})^2 \quad \text{with } \bar{s}_i = \frac{1}{n_i} \cdot \sum_{t=1}^{n_i} s_t \quad (4)$$

Where $w_{it} = L_{it} / \bar{L}_i$ ($t=1,2,.. n_i$) are the lengths of the n_i sample transects.

The global variance is estimated as

$$\hat{V}(\hat{S}) = \frac{\sum_i A_i^2 \hat{V}(\hat{S}_i)}{\left(\sum_i A_i\right)^2} \quad (5)$$

The global relative standard error of NASC

$$RSE = 100 \sqrt{\frac{\hat{V}(\hat{S})}{N}} / \hat{S} \quad (6)$$

where N is number of strata.

In order to verify acoustic observations and to analyse year class structure over the surveyed area, trawling was carried out regularly along the transects (Figure 3). All trawl stations with herring were used to derive a common length distribution for all transect within the respective strata. All stations had equal weight.

Relative standard error by number of individuals by age group was estimated by combining Monto Carlo selection from estimated NASC distributions by stratum with bootstrapping techniques of the assigned trawl stations.

The acoustic estimates presented in this report use the 38 kHz NASC, and the mean was calculated for data scrutinized as herring and collected along the transects (acoustic recordings taken during trawling, and for experimental activity are excluded). The number of herring (N) in each length group (l) within each stratum (i) is then computed as:

$$N_l = \frac{f_l \cdot \hat{S}_i \cdot A_i}{\langle \sigma \rangle}$$

Where

$$f_l = \frac{n_l L_i^2}{\sum_{l=1}^m n_l L_l}$$

is the "acoustic contribution" from the length group L_l to the total energy and $\langle s_i \rangle$ is the mean nautical area scattering coefficient [m^2/nmi^2] (NASC) of the stratum. A is the area of the stratum [nmi^2] and σ is the mean backscattering cross section at length L_l . The conversion from number of fish by length group (l) to number by age is done by estimating an age ratio from the individuals of length group (l) with age measurements. Similar, the mean weight by length and age grouped is estimated.

The mean target strength (TS) is used for the conversion where $\sigma = 4\pi 10^{(\text{TS}/10)}$ is used for estimating the mean backscattering cross section. Traditionally, $\text{TS} = 20\log L - 71.9$ (Foote 1987) has been used for mean target strength of herring during the spawning surveys, however, several papers question this mean target strength. Ona (2003) describes how the target strength of herring may change with changes with depth, due to swimbladder compression. He measured the mean target strength of herring to be $\text{TS} = 20\log L - 2.3 \log(1 + z/10) - 65.4$ where z is depth in meters. Given that previous surveys were estimated using Foote (1987), the estimation this year was also done with this TS, for direct comparison and possible inclusion in the stock assessment by ICES WGWIDE 2020 as another year in the time series.

The StoX software developed by IMR were used in the abundance estimation in 2020, just as in 2015-2019. StoX is an open source software developed at IMR, Norway (Johnsen et al. 2019) to calculate survey estimates from acoustic and swept area surveys. The program is a stand-alone application build with Java for easy sharing and further development in cooperation with other institutes. The underlying high resolution data matrix structure ensures future implementations of e.g. depth dependent target strength and high resolution length and species information collected with camera systems. Despite this complexity, the execution of an index calculation can easily be governed from user interface and an interactive GIS module, or by accessing the Java function library and parameter set using external software like R. Accessing

StoX from external software may be an efficient way to process time series or to perform bootstrapping on one dataset, where for each run, the content of the parameter dataset is altered. Various statistical survey design models can be implemented in the R-library, however, in the current version of StoX the stratified transect design model developed by Jolly and Hampton (1990) is implemented.

Sonar data and analyses

Data from Simrad low-frequency sonars were logged on board all vessels with the objective to measure the presence and magnitude of potential bias related to vertical distribution (fish in blind zone above the echo sounder transducer) and avoidance behaviour of the herring relative to the presence of the vessel. Data from fisheries sonars have been collected from all participating vessels since 2015. Methods to quantify or evaluate the extent of these biases are presently being developed.

Results and discussion

Estimates of abundance

The abundance estimates from this survey are viewed as relative, i.e. as indices of abundance, since there are highly uncertain scaling parameters like acoustic target strength and compensation for herring migrating in the opposite direction of the survey (the latter issue is discussed in Appendix 2). In StoX, there are two types of point estimates of (relative) abundance at age and total abundance: baseline estimate and mean or median based on 1000 bootstrap replications. The baseline estimates are shown in Table 1 and the bootstrap estimates are shown in Table 2. The baseline estimate of biomass from the survey is 3.24 million tonnes while the bootstrap mean estimate is 3.27 million tonnes. The decline in estimated biomass from the survey in 2019 is 24 % based on the baseline estimates and 23 % based on the bootstrap estimates. The relative standard error (CV) of the biomass estimate for 2020 based on the bootstrap replicates is 17 % which is higher than in 2019 (CV = 10 %). The survey time series of stock biomass based on bootstrap replicates from the period 2015 to 2020 is shown in Figure 4. The level of the biomass has not changed significantly during 2016-2020. The baseline estimate of total number of individuals from the survey is 12.57 billion while the bootstrap mean estimate is 12.75 billion. The decline in estimated total numbers from the survey in 2019 is 11 % based on the baseline estimates and 10 % based on the bootstrap estimates. The estimated relative standard error (CV) of the total number in 2020 based on the bootstrap replicates is 16 % which is higher than in 2019 (CV = 10 %). The survey time series of total number based on bootstrap replicates from the period 2015 to 2020 is shown in Figure 5. The level of total number has not changed significantly during 2016-2020. The estimated stock number is dominated by 4 and 7 year old herring, which is the 2016 and 2013 year classes (Table 1-2 and Figure 6). The uncertainty is high for the very young and old year classes and moderate for the most abundant ages in the survey (Table 2 and Figure 6), which is the normal pattern observed in surveys and samples from commercial catches. Estimated numbers per year class from the surveys in 2015-2020 are shown in Figure 7. The estimated numbers from the survey in 2020 seems to decline as expected for the year classes that are fully recruited to the survey, and it now seems like the survey in 2019 slightly over-estimated numbers at age (Figure 7). The 2016 year class is estimated more than three times more abundant than the 2013 year class was as 4 year olds in 2017.

Spatial distribution of the stock

The distribution and densities of herring in the area covered in 2020 was quite similar to that observed in 2017-2019, relatively evenly distributed along the coast 63-70°39'N, yet with some high density areas close to the coast from Buagrunden to Træna (63°-66°30'N) and around the continental slope outside Lofoten, the Vesterålen banks and further north (66°30'N-70°39'N) (Figure 8 and 9). The relative distribution of the estimated biomass per stratum is shown in Figure 10. Most of the biomass was found in stratum 4, 6, 7, 9 and 10, i.e. close to the coast south of Træna and on the slope around the banks outside Lofoten and Vesterålen. This distribution is fairly similar to the distribution in 2019 but a bit more uniform in 2020 with more of the biomass in the north due to the incoming 2016 year class. Age compositions per stratum are shown in Figure 11. The southernmost strata (1-4) were dominated by herring older than 6 years and the age distributions are fairly uniform. In the middle strata from Træna to Lofoten (strata 5-9) 7 year olds (2013 year class) was the most numerous while the 4 year olds (2016 year class) dominated in the northernmost strata (10-13). The 2016 year class also appears clearly in stratum 8 and 9 (outside Lofoten). Mean length and mean weight per trawl station are shown in Figure 12 and 13. These figures show that the largest herring is found in the southern part of the covered area while smaller fish dominates in the north. The observed size dependent distribution pattern in 2020 is similar to what was observed in 2015-2019 (Slotte et al 2015, 2016, 2017, 2018, 2019). It is also in accordance with the observations in earlier years, which has been thoroughly discussed in Slotte and Dommasnes, 1997, 1998, 1999, 2000; Slotte, 1998b; Slotte, 1999a, Slotte 2001, Slotte et al. 2000, Slotte & Tangen 2005, 2006).. The main hypothesis is that this could be due to the high energetic costs of migration, which is relatively higher in small compared to larger fish (Slotte, 1999b). Large fish and fish in better condition will have a higher migration potential and more energy to invest in gonad production and thus the optimal spawning grounds will be found farther south (Slotte and Fiksen, 2000), due to the higher temperatures of the hatched larvae drifting northwards and potentially better timing to the spring bloom (Vikebø et al. 2012).

Geographical variation in temperatures experienced by the herring

Temperatures experienced by herring from close to the surface and down to deeper waters than 200 m varied from 4°-8°C (Figure 14). At typical spawning depths of herring 100-200 m temperature varied more this year than in 2017-2019 (Slotte et al. 2017, 2018, 2019), with warm water in the southern part of the covered area (around 8°C), colder water west of Lofoten (4-5°C) and warmer water again furthest north (6-7°C).

Quality of the survey

In 2020 all vessels were equipped with multifrequency equipment on a drop keel. Even though the weather conditions were challenging with strong wind during most of the survey period, acoustic data with good quality was recorded and trawling on registrations could be carried out most of the time. There were some periods where the survey speed had to be reduced to ensure acceptable quality of the acoustic data. Correction for air bubble attenuation had to be done in only a few instances so most of the NASC values were not adjusted. As in earlier years, the young fish in the north was sometimes found close to the surface and it is therefore assumed that some herring was “lost” in the blind zone, especially during the night. Moreover, an unknown fraction of the 2016 year class was distributed outside the survey area (Norwegian Sea and Barents Sea). This is not unexpected as it is assumed in the ICES stock assessment that 4 year olds are not fully recruited in this survey (this information is contained in the catchability parameters). Regarding the older and larger herring in the southern part of the survey area there are no observations this year or earlier years which indicate that significant amounts of herring has been distributed outside the area covered by the survey. This issue has been extensively discussed and analysed in previous survey reports and this year it was also carried out two additional “oceanic” transect west of Buagrunnen where no herring was observed. Also, the distribution of the commercial fishery indicates that most of the spawning stock was contained in the area covered by the survey. To conclude, the acoustic and biological data recorded in 2020 were of satisfactory quality and the estimates from the survey are recommended to be used in the stock assessment of Norwegian spring-spawning herring.

References

- Demer, D.A., Berger, L., Bernasconi, M., Bethke, E., Boswell, K., Chu, D., Domokos, R., *et al.* 2015. Calibration of acoustic instruments. ICES Cooperative Research Report No. 326. 133 pp.
- Foote, K. 1987. Fish target strengths for use in echo integrator surveys. *J. Acoust. Soc. Am.* 82: 981-987.
- Harbitz, A. 2019. A zigzag survey design for continuous transect sampling with guaranteed equal coverage probability. *Fisheries Research* 213, 151-159.
- Johnsen, E., Totland, A., Skålevik, Å., Holmin, A.J., Dingsør, G.E., Fuglebakk, E., Handegard, N.O. 2019. StoX: An open source software for marine survey analyses. *Methods in Ecology and Evolution* 10:1523–1528.
- Jolly, G.M., and Hampton, I. 1990. A stratified random transect design for acoustic surveys of fish stocks. *Canadian Journal of Fisheries and Aquatic Sciences* 47: 1282-1291.

- Korneliussen, R. J., and Ona, E. 2002. An operational system for processing and visualizing multi-frequency acoustic data. *ICES Journal of Marine Science*, 59: 293–313.
- Korneliussen, R. J., Ona, E., Eliassen, I., Heggelund, Y., Patel, R., Godø, O.R., Giertsen, C., Patel, D., Nornes, E., Bekkvik, T., Knudsen, H.P., Lien, G. The Large Scale Survey System - LSSS. Proceedings of the 29th Scandinavian Symposium on Physical Acoustics, Ustaoset 29 January– 1 February 2006.
- MacLennan, D.N., Fernandes, P., and Dalen, J. 2002. A consistent approach to definitions and symbols in fisheries acoustics. *ICES J. Mar. Sci.*, 59: 365-369.
- Ona, Egil. 1999. An expanded target-strength relationship for herring. "ICES Journal of Marine Science: Journal du Conseil 60: 493-499.
- Ona, E. (Ed). 1999. Methodology for target strength measurements (with special reference to *in situ* techniques for fish and mikro-nekton. ICES Cooperative Research Report No. 235. 59 pp.
- Simmonds, J, and David N. MacLennan. 2005. Fisheries acoustics: theory and practice. John Wiley & Sons, 2008.
- Slotte, A. 1998a. Patterns of aggregation in Norwegian spring spawning herring (*Clupea harengus* L.) during the spawning season. *ICES C. M.* 1998/J:32.
- Slotte, A. 1998b. Spawning migration of Norwegian spring spawning herring (*Clupea harengus* L.) in relation to population structure. Ph. D. Thesis, University of Bergen, Bergen, Norway. ISBN : 82-7744-050-2.
- Slotte, A. 1999a. Effects of fish length and condition on spawning migration in Norwegian spring spawning herring (*Clupea harengus* L.). *Sarsia* **84**, 111-127.
- Slotte, A. 1999b. Differential utilisation of energy during wintering and spawning migration in Norwegian spring spawning herring. *Journal of Fish Biology* **54**, 338-355.
- Slotte, A. 2001. Factors Influencing Location and Time of Spawning in Norwegian Spring Spawning Herring: An Evaluation of Different Hypotheses. In: F. Funk, J. Blackburn, D. Hay, A.J. Paul, R. Stephenson, R. Toresen, and D. Witherell (eds.), *Herring: Expectations for a New Millennium*. University of Alaska Sea Grant, AK-SG-01-04, Fairbanks, pp. 255-278.
- Slotte, A. and Dommasnes, A. 1997. Abundance estimation of Norwegian spring spawning at spawning grounds 20 February-18 March 1997. Internal cruise reports no. 4. Institute of Marine Research, P.O. Box. 1870. N-5024 Bergen, Norway.
- Slotte, A. and Dommasnes, A. 1998. Distribution and abundance of Norwegian spring spawning herring during the spawning season in 1998. *Fisken og Havet* **5**, 10 pp.
- Slotte, A. and Dommasnes, A. 1999. Distribution and abundance of Norwegian spring spawning herring during the spawning season in 1999. *Fisken og Havet* **12**, 27 pp.
- Slotte, A and Dommasnes, A. 2000. Distribution and abundance of Norwegian spring spawning herring during the spawning season in 2000. *Fisken og Havet* **10**, 18 pp.
- Slotte, A. and Fiksen, Ø. 2000. State-dependent spawning migration in Norwegian spring spawning herring (*Clupea harengus* L.). *Journal of Fish Biology* **56**, 138-162.
- Slotte, A. & Tangen, Ø. 2005. Distribution and abundance of Norwegian spring spawning herring in 2005. Institute of Marine Research, P. O. Box 1870 Nordnes, N-5817 Bergen (www.imr.no). ISSN 1503-6294/Cruise report no. 4 2005.

- Slotte, A. and Tangen, Ø. 2006. Distribution and abundance of Norwegian spring spawning herring in 2006. Institute of Marine Research, P. O. Box 1870 Nordnes, N-5817 Bergen (www.imr.no). ISSN 1503-6294/Cruise report no. 1. 2006.
- Slotte, A., Johannessen, A and Kjesbu, O. S. 2000. Effects of fish size on spawning time in Norwegian spring spawning herring (*Clupea harengus* L.). Journal of Fish Biology 56: 295-310.
- Slotte A., Johnsen, E., Pena, H., Salthaug, A., Utne, K. R., Anthonypillai, A., Tangen , Ø and Ona, E. 2015. Distribution and abundance of Norwegian spring spawning herring during the spawning season in 2015. Survey report / Institute of Marine Research/ISSN 1503 6294/Nr. 5 – 2015
- Slotte, A., Salthaug, A., Utne, KR, Ona, E., Vatnehol, S and Pena, H. 2016. Distribution and abundance of Norwegian spring spawning herring during the spawning season in 2016. Survey report / Institute of Marine Research/ /ISSN 1503 6294/Nr. 17–2016
- Slotte, A., Salthaug, A., Utne, KR, Ona, E. 2017. Distribution and abundance of Norwegian spring spawning herring during the spawning season in 2017. Survey report / Institute of Marine Research/ ISSN 15036294/Nr. 8 – 2017
- Slotte A., Salthaug, A., Høines, Å., Stenevik E. K., Vatnehol, S and Ona, E. 2018. Distribution and abundance of Norwegian spring spawning herring during the spawning season in 2018. Survey report / Institute of Marine Research/ISSN 15036294/Nr. 5– 2018.
- Slotte, A., Salthaug, A., Stenevik, E.K., Vatnehol, S. and Ona, E. 2019 Distribution and abundance of Norwegian spring spawning herring during the spawning season in 2019. Survey report / Institute of Marine Research/ISSN 15036294/Nr. 2– 2018.
- Vikebø, F., Korosov, A., Stenevik, E.K., Husebø, Å. Slotte, A. 2012. Spatio-temporal overlap of hatching in Norwegian spring spawning herring and spring phytoplankton bloom at available spawning substrates – observational records from herring larval surveys and SeaWIFS. ICES Journal of Marine Science, 69: 1298-1302.

Tables

Table 1. Baseline estimates from StoX of Norwegian spring-spawning herring during the spawning season 14.-26. February 2020.

Length (cm)	age																		Number	Biomass	MeanW		
	2	3	4	5	6	7	8	9	10	11	12	13	14	15	16	17	18	Unknown					
21-22	4401	-	-	-	-	-	-	-	-	-	-	-	-	-	-	-	-	-	-	4401	264	60	
22-23	-	-	-	-	-	-	-	-	-	-	-	-	-	-	-	-	-	-	-	-	-	-	
23-24	-	-	-	-	-	-	-	-	-	-	-	-	-	-	-	-	-	-	-	5970	5970	501	83.9
24-25	-	-	24672	-	-	-	-	-	-	-	-	-	-	-	-	-	-	-	-	-	24672	2143	86.8
25-26	-	3349	79838	-	-	-	-	-	-	-	-	-	-	-	-	-	-	-	-	-	83187	8304	99.8
26-27	-	6738	226706	8151	-	-	-	-	-	-	-	-	-	-	-	-	-	-	-	-	241595	28037	116.1
27-28	-	16462	560050	2246	-	-	-	-	-	-	-	-	-	-	-	-	-	-	-	-	578758	74175	128.2
28-29	-	4401	1042950	78583	15729	38580	-	-	-	-	-	-	-	-	-	-	-	-	-	-	1180245	172641	146.3
29-30	-	8803	851130	57312	23250	-	-	-	34397	-	-	-	-	-	-	-	-	-	-	-	974892	160763	164.9
30-31	-	-	412161	124936	62859	-	-	-	-	-	-	-	-	-	-	-	-	-	-	-	599956	113719	189.6
31-32	-	-	124488	136422	323548	272276	2332	2896	-	-	-	-	-	-	-	-	-	-	-	-	861962	194614	225.8
32-33	-	-	52436	51801	485479	947774	47440	3088	-	-	-	-	-	-	-	-	-	-	-	-	1588018	403094	253.8
33-34	-	-	20670	55790	283548	1221070	176018	76803	-	-	-	-	-	-	-	-	-	-	-	-	1833899	505588	275.7
34-35	-	-	-	24537	33764	607968	174940	202273	19902	23515	4666	9854	9903	-	20635	-	-	-	-	-	1131956	340265	300.6
35-36	-	-	33467	-	22277	207402	72637	191609	63650	193184	24543	35361	117013	58179	89862	-	2399	-	-	-	1111581	371008	333.8
36-37	-	-	-	-	-	20699	35799	57267	124742	350808	66818	143322	311285	51094	224322	39112	8180	-	-	-	1433447	510053	355.8
37-38	-	-	-	-	1714	10637	7449	31916	65666	99504	20180	50587	210310	21927	166959	36004	1253	-	-	-	724106	276079	381.3
38-39	-	-	-	-	-	-	-	6200	7978	3720	6628	30840	40734	9932	27522	1845	29247	-	-	-	164645	66541	404.2
39-40	-	-	-	-	-	-	-	-	-	-	-	-	-	-	6586	-	10496	-	-	-	17081	7374	431.7
40-41	-	-	-	-	-	-	-	-	-	-	-	-	2079	-	5669	-	-	-	-	-	7748	3893	502.4
TSN (1000)	4401	39752	3428570	539777	1252169	3326407	516615	572050	316334	670730	122835	269964	691324	141131	541554	76960	51575	5970	12568119	-	-	-	
TSB (t)	264	5428	532007	109415	304172	917088	153727	184640	106128	237339	44483	97099	249981	51076	197450	28077	20182	501	-	-	3239055	-	
Mean L (cm)	21.5	27.4	28.6	30.7	32.2	33.1	34.1	34.9	35.4	36.0	36.2	36.4	36.5	36.1	36.5	36.8	38.0	23.5	-	-	-	-	
Mean W (g)	60.0	136.5	155.2	202.7	242.9	275.7	297.6	322.8	335.5	353.9	362.1	359.7	361.6	361.9	364.6	364.8	391.3	83.9	-	-	-	257.7	
% mature	0	72	97	100	100	100	100	100	100	100	100	100	100	100	100	100	100	100	-	-	-	-	
SSB (t)	0	3908	516047	109415	304172	917088	153727	184640	106128	237339	44483	97099	249980	51076	197450	28077	20182	-	-	-	-	3220811	

Table 2. Bootstrap estimates from StoX (based on 1000 replicates) of Norwegian spring-spawning herring during the spawning season 14. -26. February 2020. Numbers by age and total number (TSN) are in millions and total biomass (TSB) in thousand tons.

Age	5th percentile	Median	95th percentile	Mean	SD	CV
2	0.0	4.0	19.3	5.7	6.7	1.17
3	9.7	38.6	104.5	44.4	29.7	0.67
4	2385.5	3427.1	4808.1	3502.4	741.0	0.21
5	354.9	552.4	840.6	571.1	152.8	0.27
6	847.4	1202.5	1602.0	1212.4	225.7	0.19
7	2363.1	3329.1	4307.9	3336.7	584.4	0.18
8	349.3	523.9	729.3	530.2	116.2	0.22
9	406.4	599.6	850.5	609.1	135.1	0.22
10	201.8	355.4	553.2	364.1	109.5	0.30
11	415.7	641.6	919.5	649.7	154.0	0.24
12	80.2	127.9	192.7	131.4	34.9	0.27
13	177.6	273.8	393.1	279.5	67.2	0.24
14	384.6	669.7	987.6	676.6	187.1	0.28
15	64.2	152.3	258.9	154.9	59.3	0.38
16	330.6	520.8	843.4	541.4	153.8	0.28
17	42.8	76.2	134.9	81.0	27.2	0.34
18	10.9	46.7	95.6	48.1	26.9	0.56
TSN	9375.3	12756.7	16221.0	12750.4	2068.2	0.16
TSB	2376.8	3269.2	4212.5	3273.7	543.9	0.17

Figures

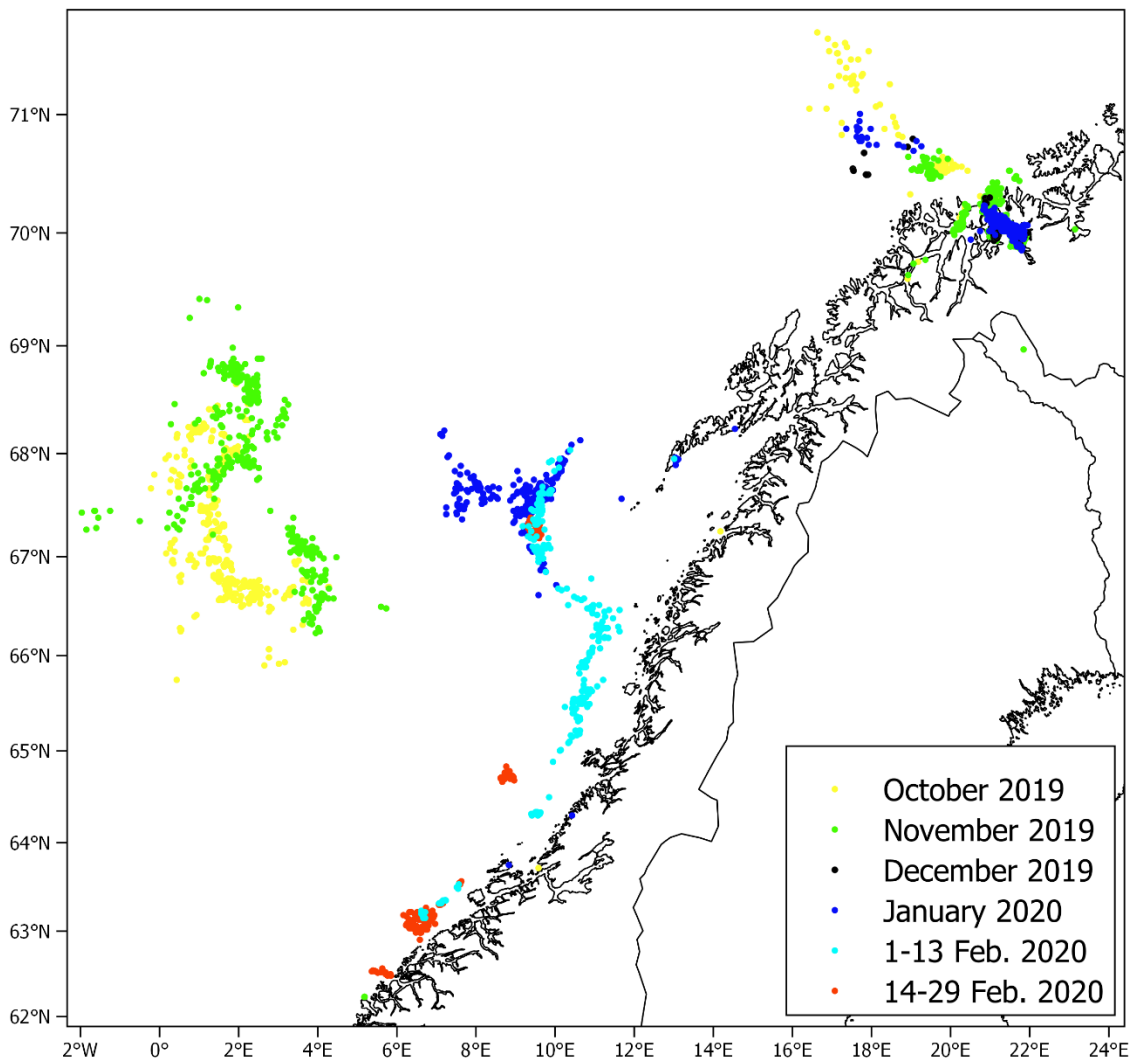


Figure 1. Distribution of commercial catches of Norwegian Spring-spawning herring from October 2019 until February 2020, based on electronic logbooks. Each point represent one catch, only catches larger than 10 tons are shown.

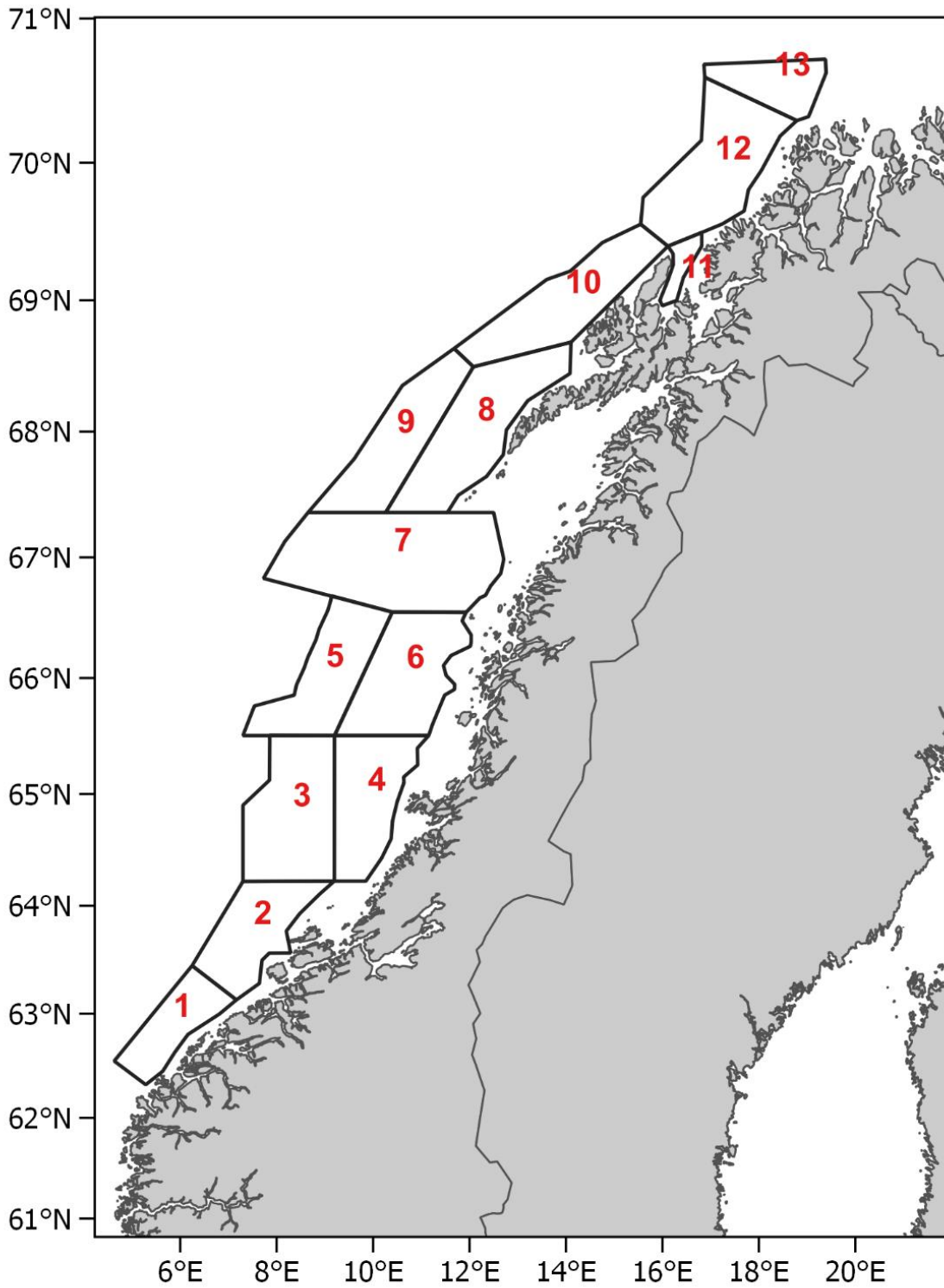


Figure 2. Strata covered during 14.-26. February 2020 with MS *Eros*, *Kings Bay* and *Vendla*

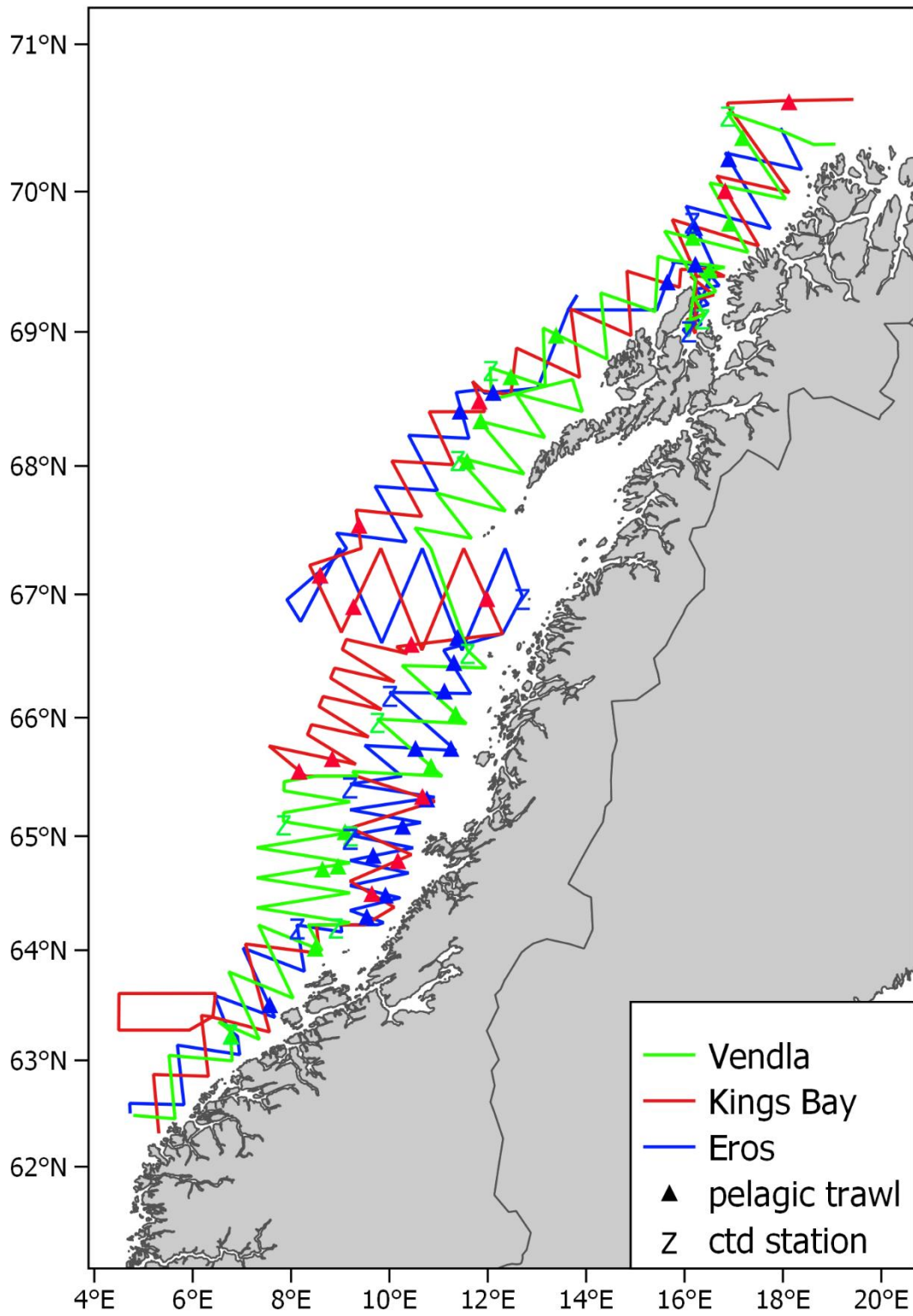


Figure. 3. Acoustic transects, pelagic trawl stations (triangles), and CTD stations (Z) covered with *Eros*, *Kings Bay* and *Vendla* 14.-26. February 2020.

SPAWNING SURVEY, TSB

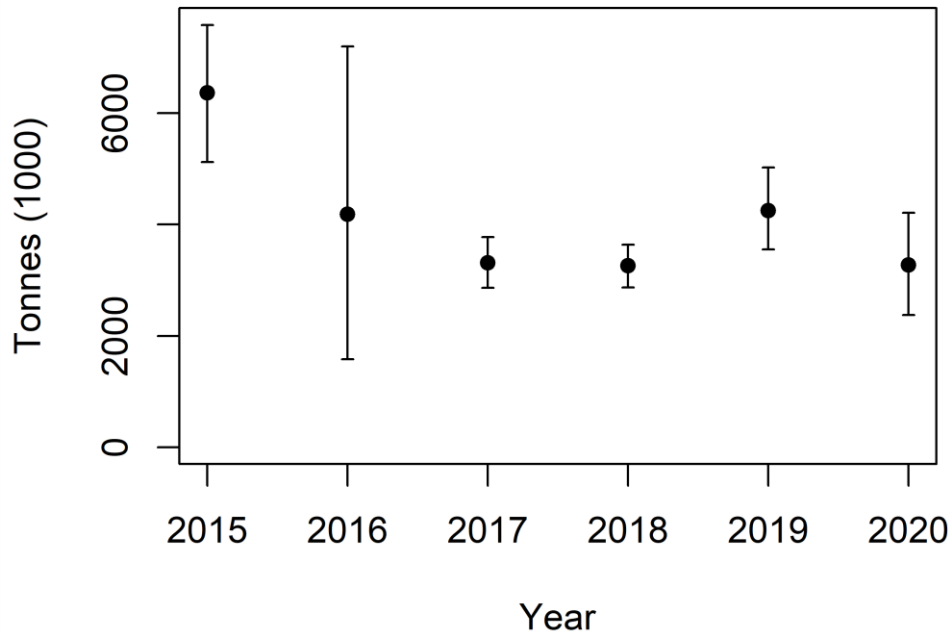


Figure 4. Estimates of total biomass from the Norwegian spring-spawning herring spawning surveys 2015-2020. The estimates are mean of 1000 bootstrap replicates in StoX and the error bars represent 90 % confidence intervals.

SPAWNING SURVEY, TSN

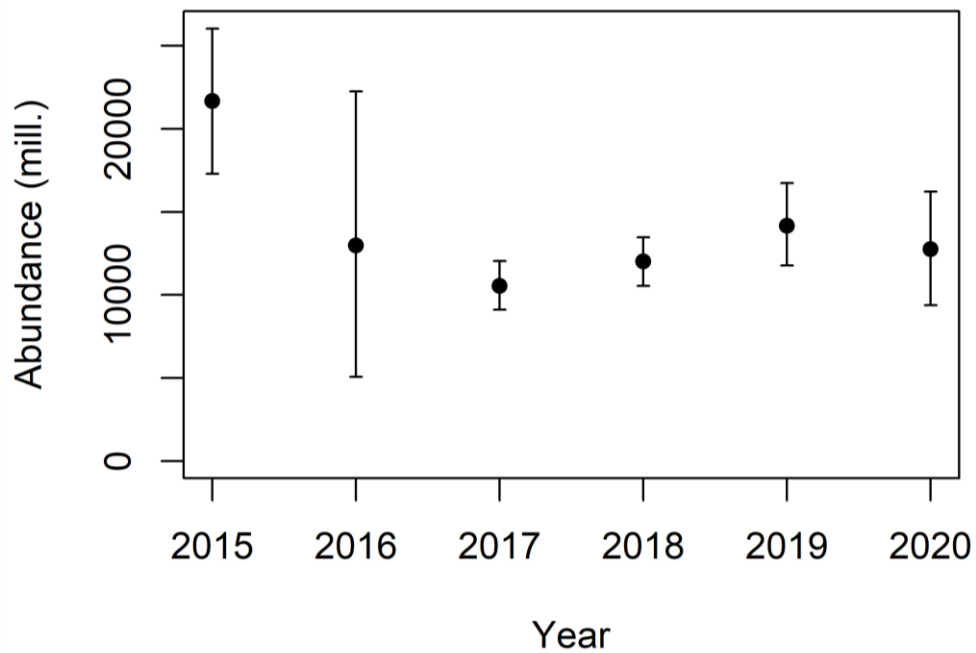


Figure 5. Estimates of total number from the Norwegian spring-spawning herring spawning surveys 2015-2020. The estimates are mean of 1000 bootstrap replicates in StoX and the error bars represent 90 % confidence intervals.

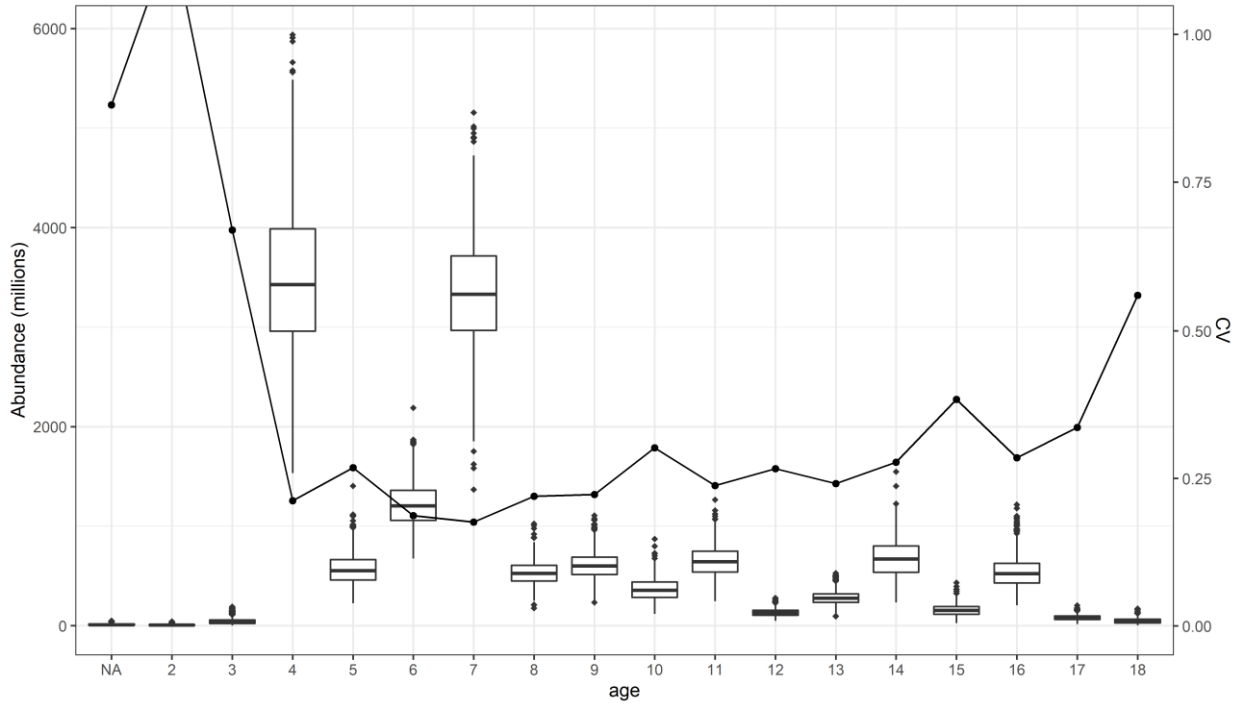


Figure 6. Standard box plot of abundance by age with uncertainty (CV) as estimated during 14.-26. February 2020. The Uncertainty estimates were based on 1000 bootstrap replicates in StoX.

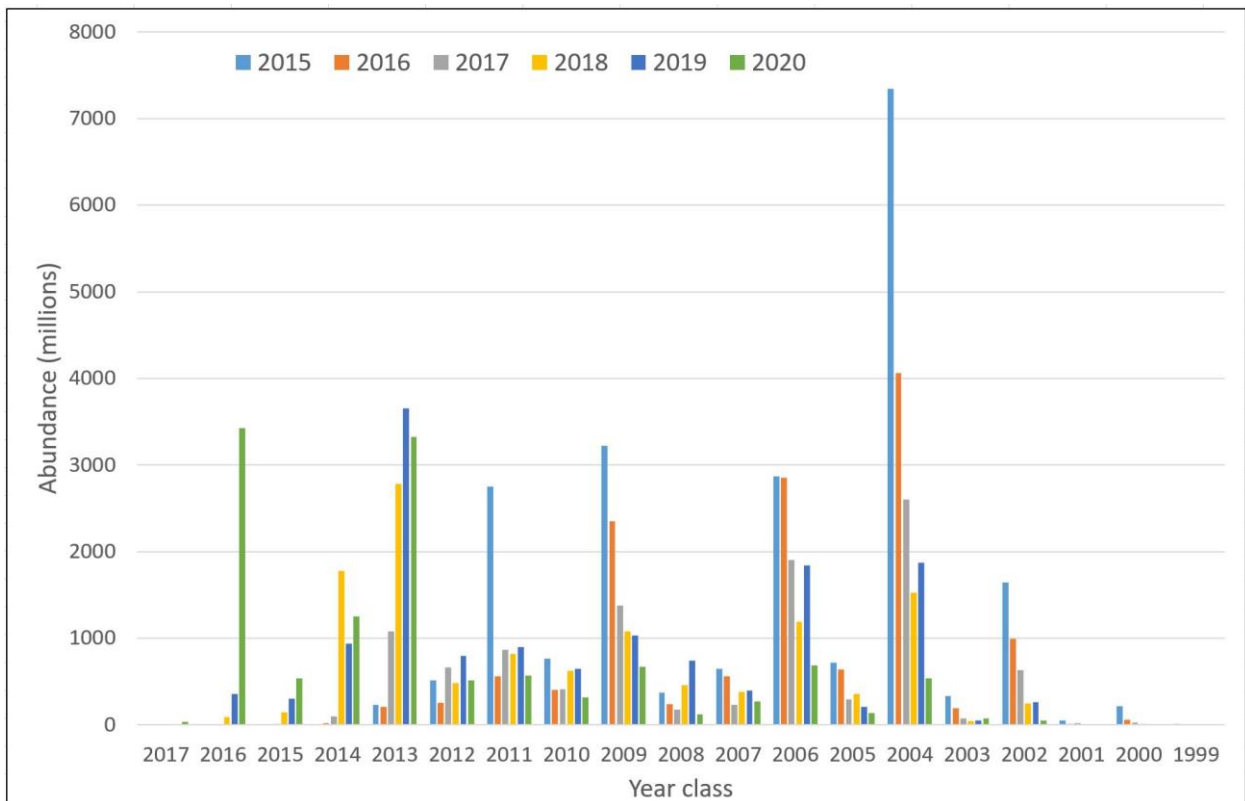


Figure 7. Abundance by year class estimated during the Norwegian spring-spawning herring surveys 2015-2020 (baseline estimates from StoX). Legend: Separate colour for each survey year.

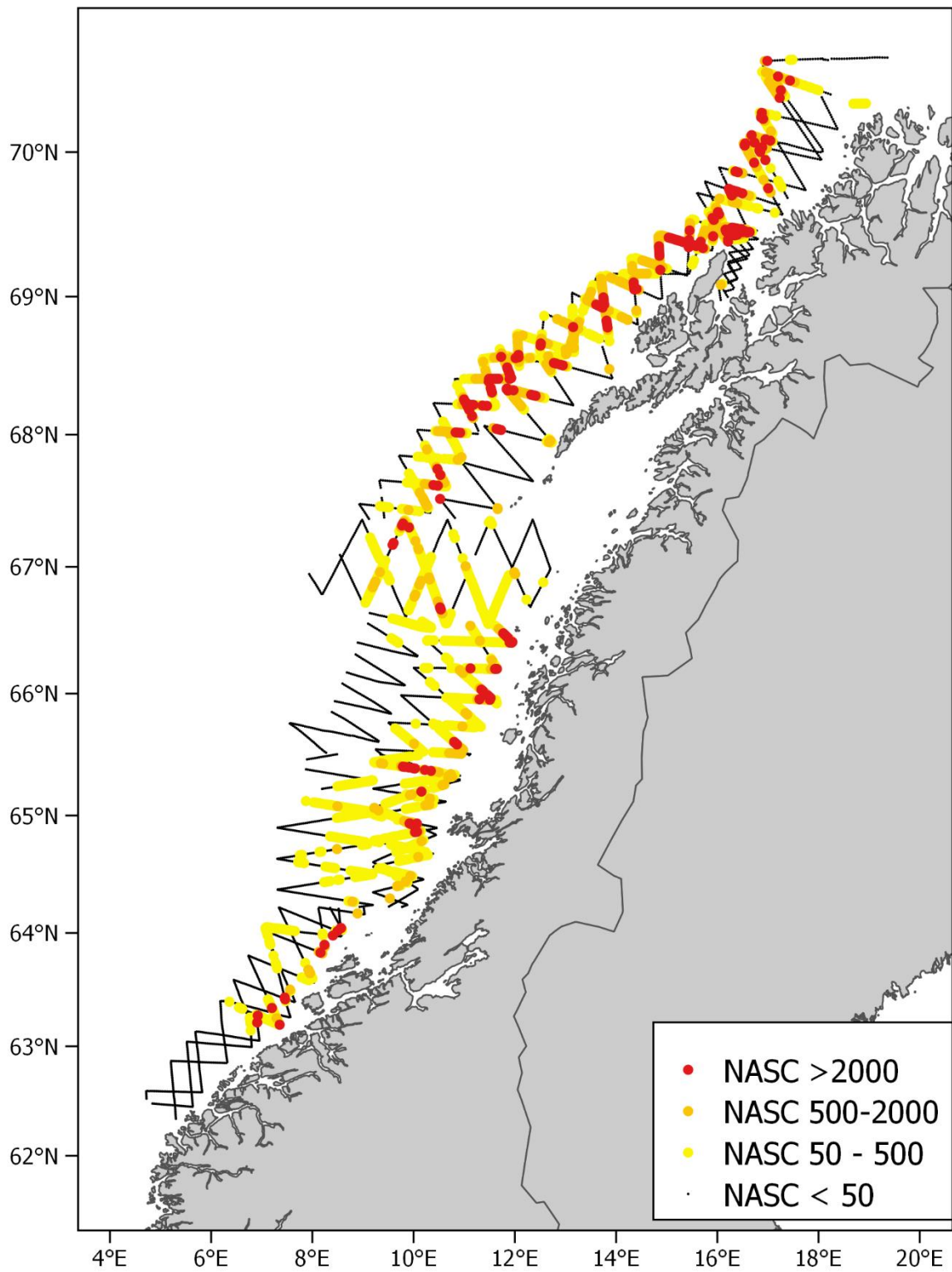


Figure 8. Acoustic density (NASC) of herring recorded during 14.-26. February 2020. Points represent NASC values per nautical mile.

+

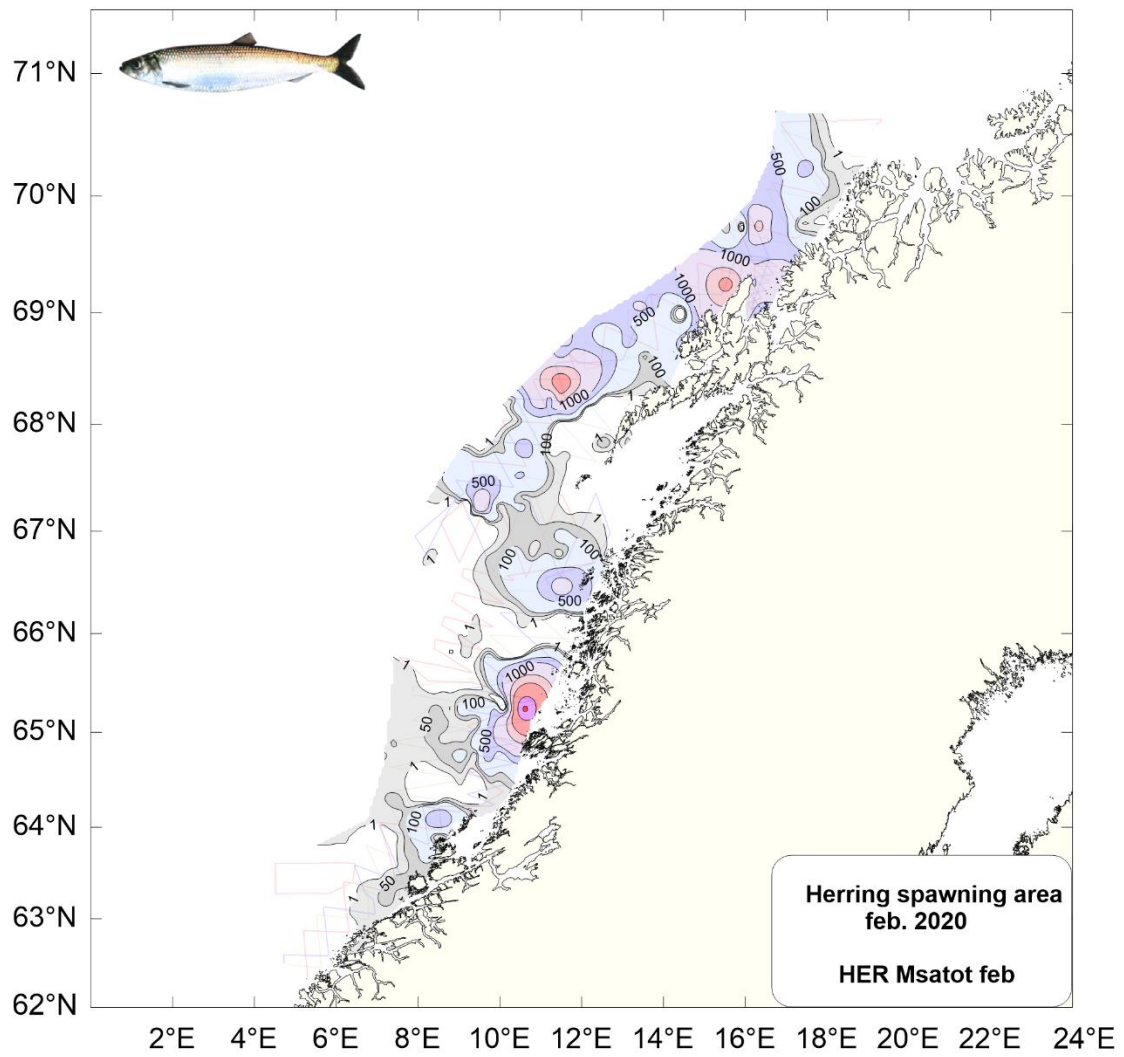


Figure 9. Contour plot of acoustic density (NASC) of herring recorded during 14.-26. February 2020.

+

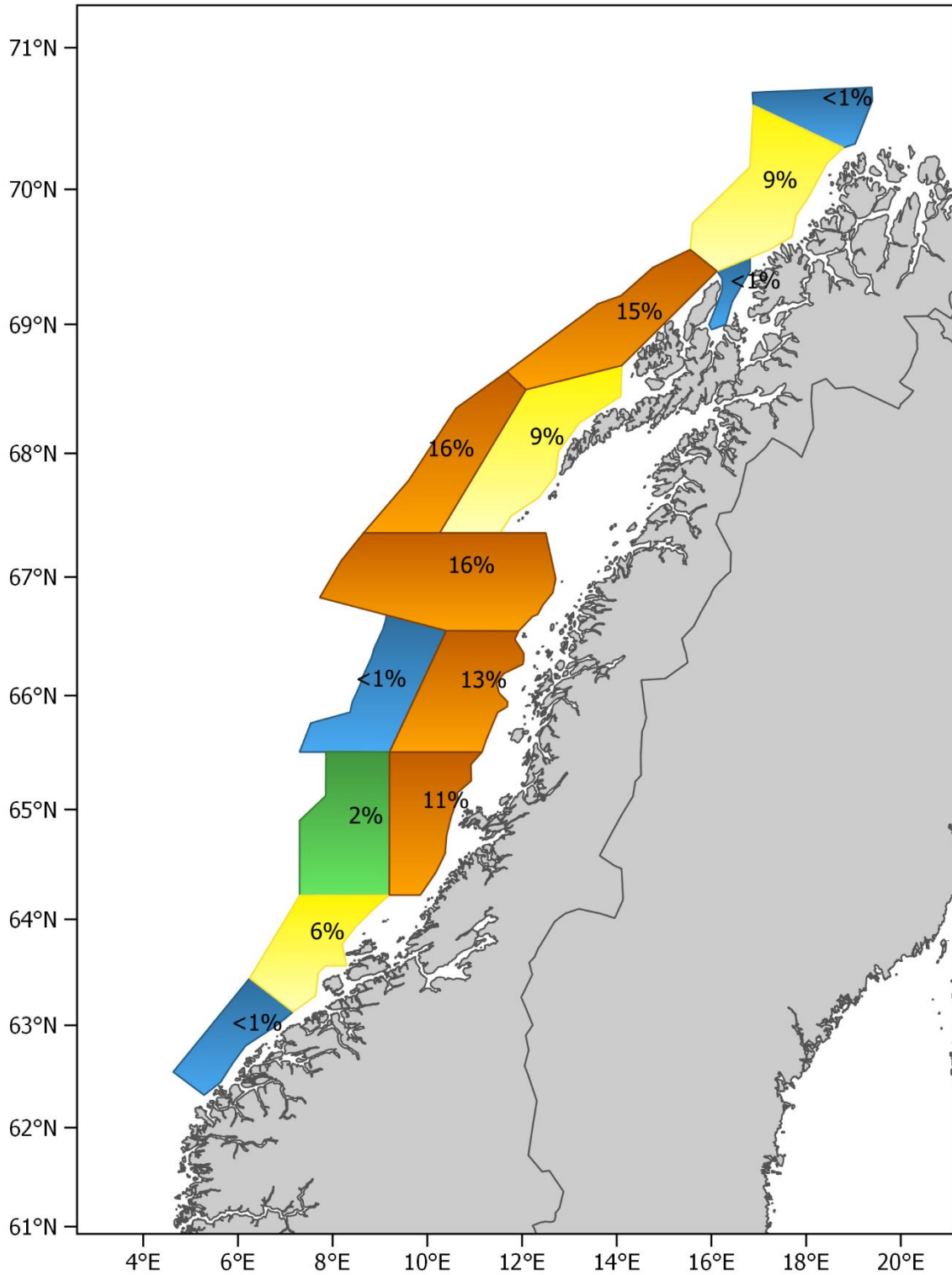


Figure. 10. Relative distribution by stratum of the biomass of herring (baseline estimates from StoX) 14.-26. February 2020. Strata numbers are given in Figure 2.

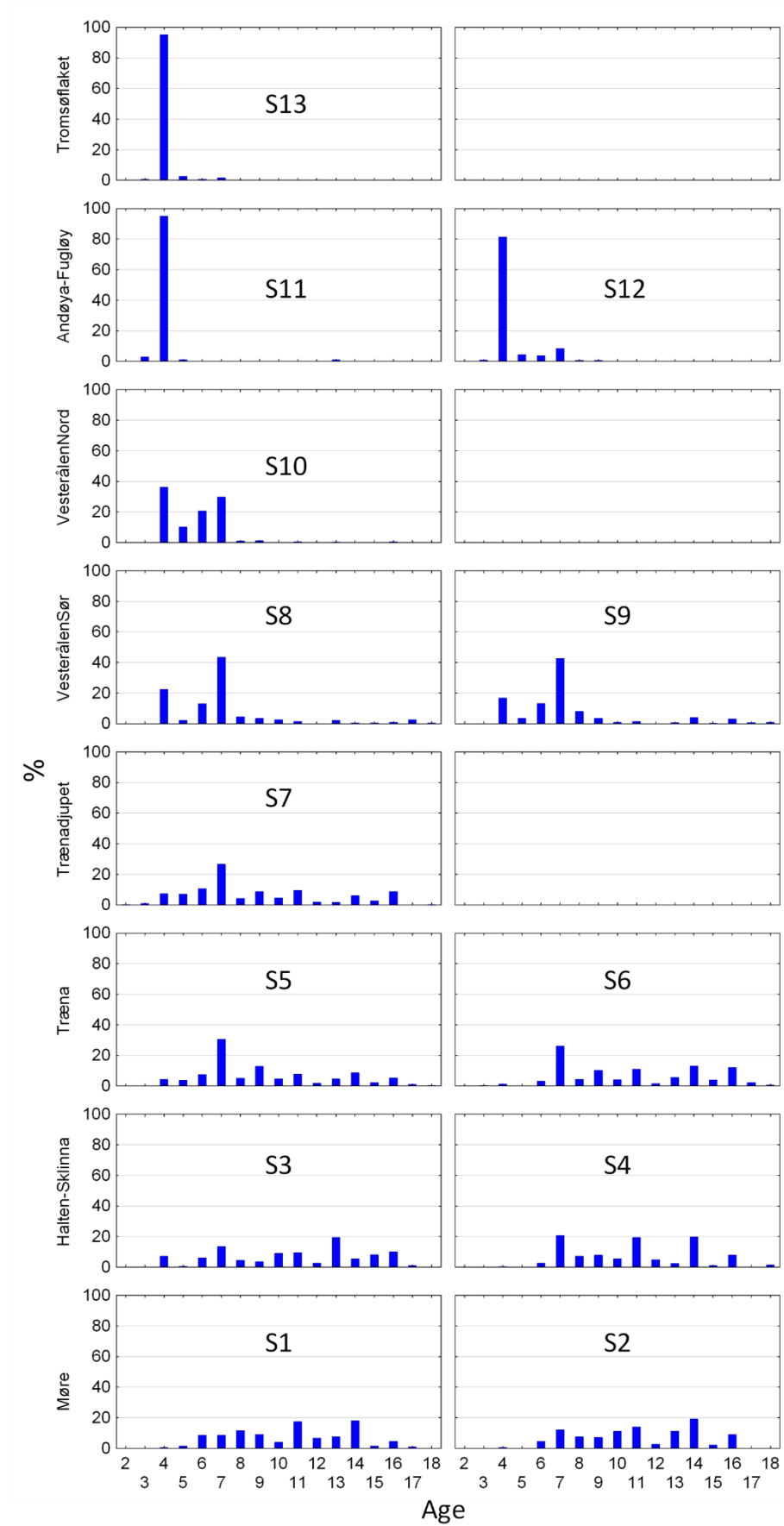


Figure 11. Comparison of age composition (%) estimated in different strata covered during 14.-26. February 2020. Strata numbers are given in Figure 2.

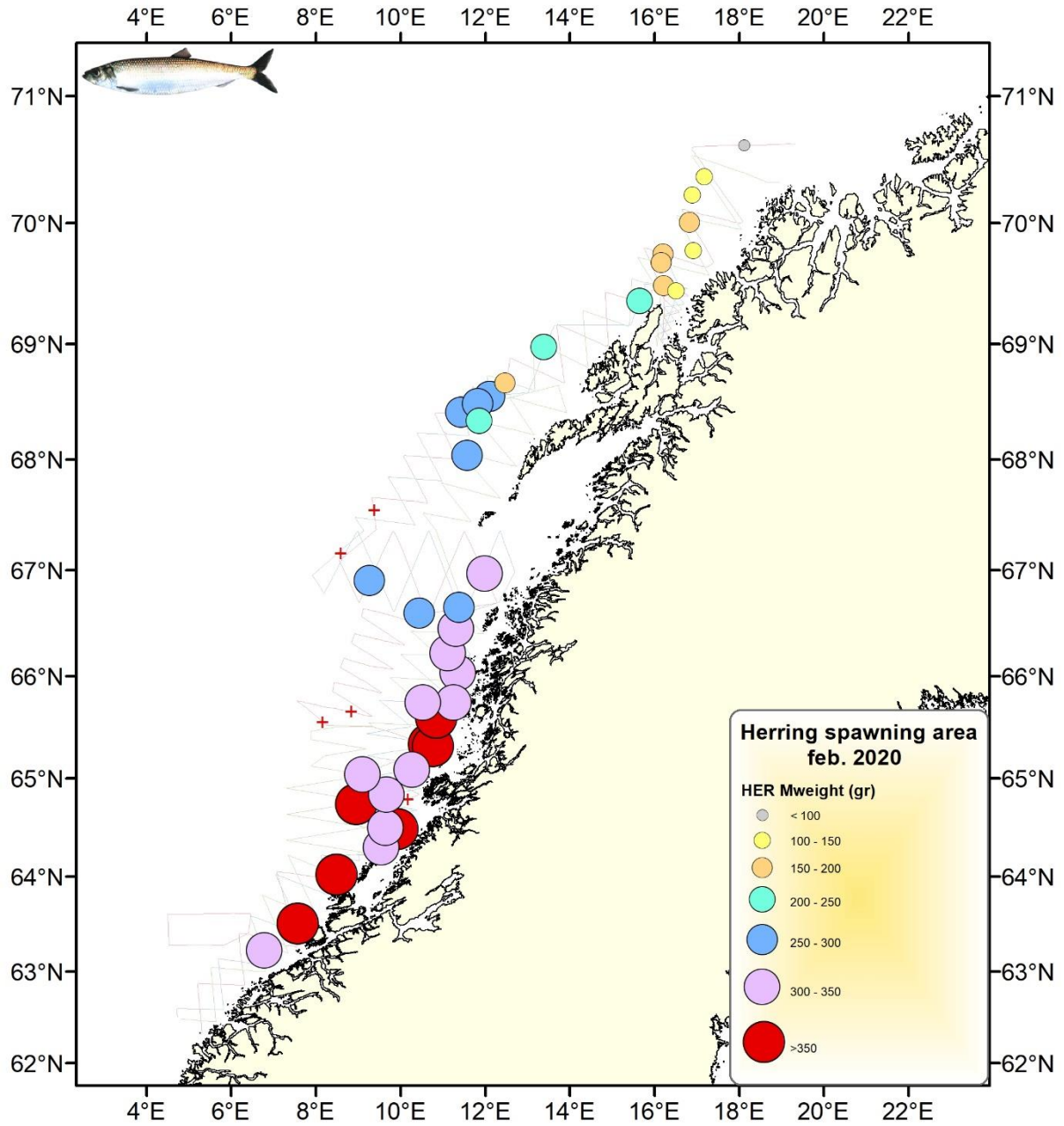


Figure 12. Mean weight (g) of herring by trawl station during the Norwegian spring-spawning herring survey 14.-26. February 2020.

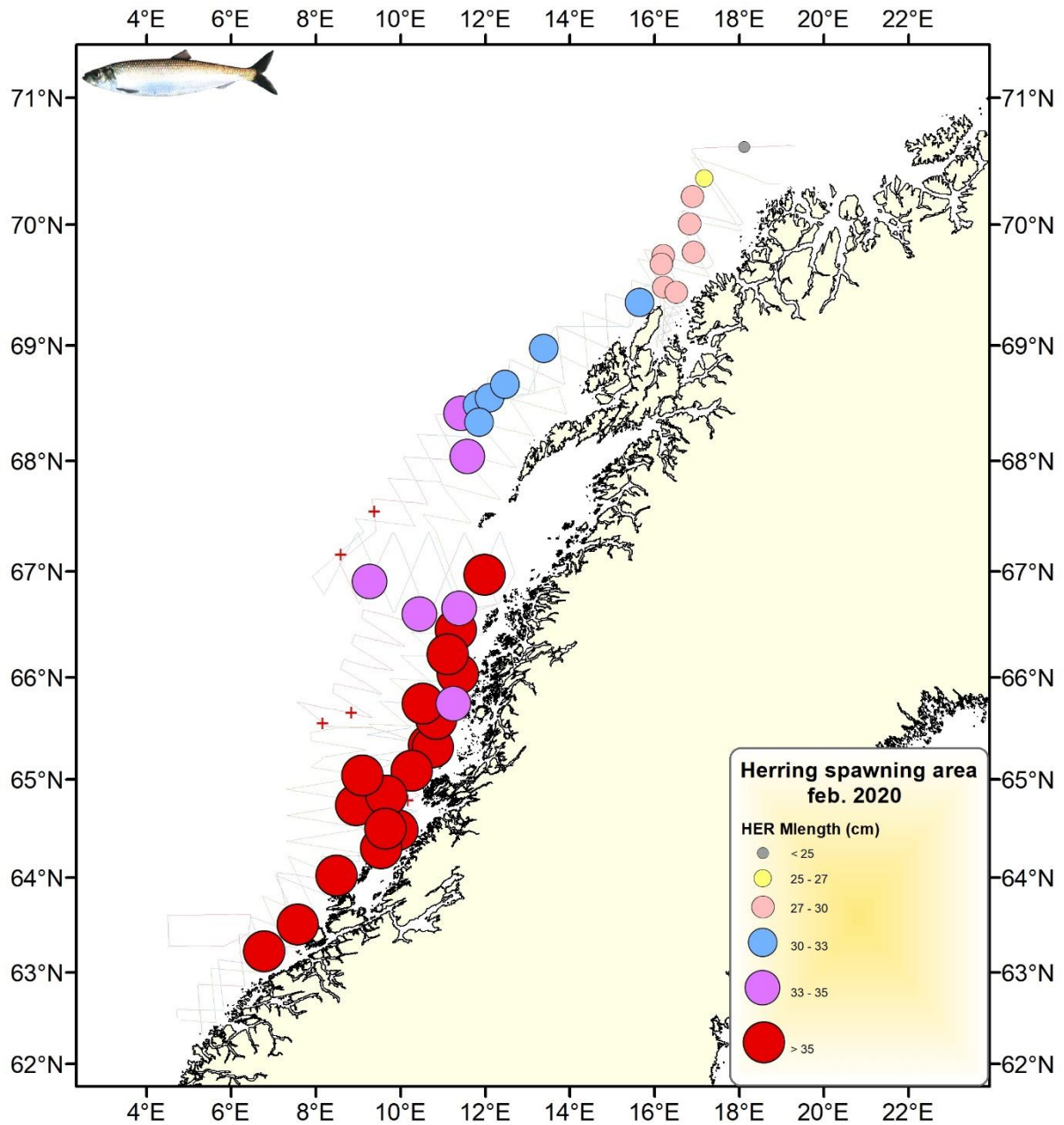


Figure 13. Mean length (cm) of herring by trawl station during the Norwegian spring-spawning herring survey 14.-26. February 2020.

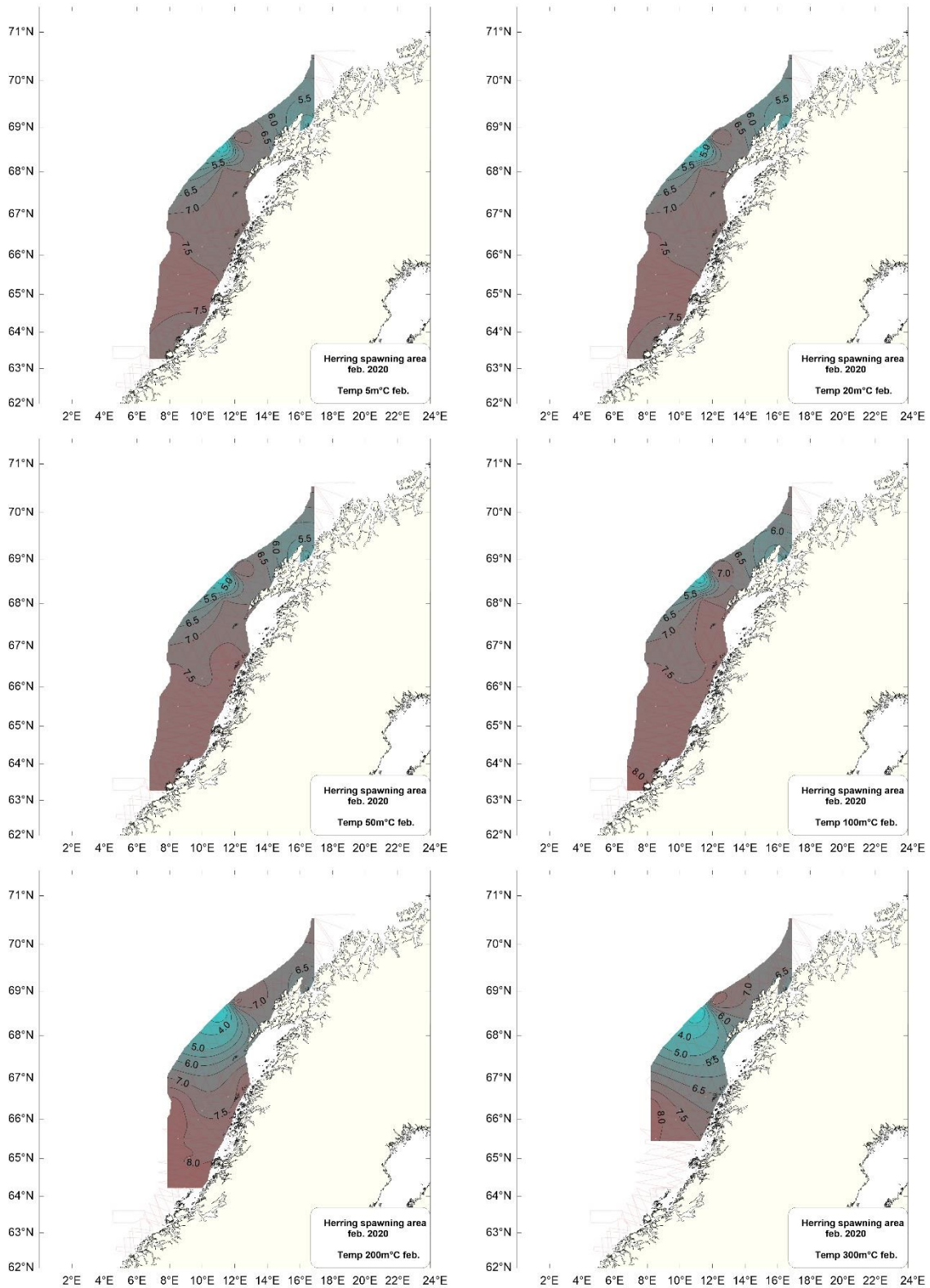


Figure 14. Temperature at 5, 20, 50, 100, 200, 300 m in the area covered during the Norwegian spring-spawning herring survey 14.-26. February 2020.

Annex 1. Calibration results and settings

Table 1. Calibration data and parameter settings of the five echo sounders on each survey vessel in the survey, with the calibration done on February 14, 2020. Kings Bay has Simrad EK80 WBT's, while Vendla and EROS has Simrad EK60. EROS is running the EK80 software on the EK60 GPT's, while VENDLA runs the original EK60 software. The new WC57.2 calibration sphere was as target for all frequencies when calibrated at the tip of the fishery pier in Ålesund, with tabulated values for the sphere TS on EK60, and with the internally computed by the calibration program in EK80. After calibration was accepted, the new calibration parameters were entered into the echo sounders. The validity of the WC 57.2 calibration sphere against the original CU60 at 38 kHz was previously conducted on G.O.Sars in November 2018 with good results. The echo sounders calibration showed very good stability compared to 2017 and 2018. The 200 Khz echo sounder on Kings Bay was changed due to the failure discovered in 2018, and the 38 kHz system was changed due to a ripping of the old transducer cable. Otherwise, the systems are very stable, and as an example the calibration of the Vendla EK60 system gave values within 0.1 dB from previous February 2019 calibration except for 200 kHz, where the difference was 0.2 dB.

MS Kings Bay, Simrad EK80

Parameter	Survey data sample 2020818 1402: Simrad EK80, CW, 1 ms				
Transducer type	ES18	ES38-7	ES70-7C	ES120-7C	ES200-7C
Transmission frequency [kHz]	18	38	70	120	200
Transmission power [W]	2000	2000	750	250	150
Pulse duration [ms]	1.024	1.024	1.024	1.024	1.024
TS Transducer Gain [dB]	23.06	26.33	27.76	27.27	26.58
Sa Correction (dB)	0.009	0.000	0.16	-0.20	-0.33
Equivalent beam angle [dB]	-17.0	-20.7	-20.7	-20.7	-20.7
Absorption coefficient [dB km ⁻¹]	2.9	10.1	20.9	31.8	52.15
Half power beam widths (along/athwart ship) [deg]	9.77/9.87	5.5/4.9	6.71/6.68	6.27/6.61	7.20/6.90
Transducer angle sensitivity (along ship and athwart ship)	15.5	23.0	23.0	23.0	23.0
Sound speed [m s ⁻¹]	1473	1473	1473	1473	1473

M/S Vendla, Simrad EK60

Parameter	Calibration 20190218 Simrad EK60, CW narrow-band				
Transducer type	ES18	ES38B	ES70-7C	ES120-7C	ES200-7C
Transmission frequency [kHz]	18	38	70	120	200
Transmission power [W]	2000	2000	750	250	120
Pulse duration [ms]	1.024	1.024	1.024	1.024	1.024
TS Transducer Gain [dB]	22.84	25.46	26.53	27.09	27.25
Sa Correction (dB)	-0.57	-0.72	-0.35	-0.27	-0.27
Equivalent beam angle [dB]	-17.0	-20.6	-20.7	-21.0	-20.7
Absorption coefficient [dB km ⁻¹]	2.8	9.6	20.3	31.3	44.5

Half power beam widths (along/athwart ship) [deg]	10.81/10.86	6.97/7.05	6.53/6.62	6.44/6.56	6.59/6.31
Transducer angle sensitivity (along ship and athwart ship)	15.5	23.0	23.0	23.0	23.0
Sound speed [m s^{-1}]	1471	1471	1471	1471	1471

M/S EROS, Simrad EK60

Parameter	Calibration 20180218, Simrad EK60, CW narrow-band				
	ES18	ES38B	ES70-7C	ES120-7C	ES200-7C
Transducer type	ES18	ES38B	ES70-7C	ES120-7C	ES200-7C
Transmission frequency [kHz]	18	38	70	120	200
Transmission power [W]	2000	2000	375	150	90
Pulse duration [ms]	1.024	1.024	1.024	1.024	1.024
TS Transducer Gain [dB]	22.25	25.84	26.52	26.67	26.53
SaCorrection [dB]	-0.23	0.00	-0.33	-0.36	-0.26
Equivalent beam angle [dB]	-17.0	-20.6	-20.7	-21.0	-20.7
Absorption coefficient [dB km^{-1}]	2.8	9.7	20.6	31.6	44.9
Half power beam widths (along/athwart ship) [deg]	10.15/10.32	6.99/6.80	6.86/6.92	6.97/6.70	6.03/5.79
Transducer angle sensitivity (along ship and athwart ship)	15.5	23.0	23.0	23.0	23.0
Sound speed [m s^{-1}]	1473	1473	1473	1473	1473

February 25. 2020, Egil Ona, M/S EROS, at Sea

Annex 2. Measuring the migration speed of herring

The spawning survey on NVG herring along the Norwegian coast is designed as a snap-shot survey over 12 days, covering a survey area of 30443 nmi². A zig zag survey design gives a higher mean progress speed than parallel transects (Harbiz, 2019). However, before spawning, the herring migrate against the prevailing current direction, and actively use the tidal variations in the current to adjust the migration speed. Vertical positioning therefore seems to be important. Simmonds and MacLennan (2005) writes: “The movements of fish can be conceived as having two components, random motion and migration. In the former case, the fish swim at a certain speed in directions that change randomly with time. In the latter case, the fish swim consistently in the same direction. Simmonds *et al.* (2002) used a fine-scale model of North Sea herring schools, based on a spatial grid covering 120 000 km² with a node spacing of 40 m, to study the effect of fish movements on the results of simulated surveys. They found that the random motion was unimportant, but the effect of systematic migration even at a modest speed could not be ignored. One factor in the survey design is the timing in relation to the migration cycle, which should ensure that the surveyed area includes the entire stock. But even if this condition is met, migration of the stock within the surveyed area can bias the abundance estimate. The extent of the bias depends on the direction of the migration in relation to the transects. Suppose the fish are migrating at speed v_f , and v_s is the speed at which the survey progresses in the direction of migration. If v_s is positive, this means that the fish tend to follow the vessel as it travels along successive transects. If the cruise track were drawn on a map whose frame of reference moved with the fish, the transects would be closer together than those on the geostationary map. Thus the effective area applicable to the analysis is less than the actual area surveyed. The observed densities are unbiased, but since the abundance is the mean density multiplied by the effective area, the estimate \hat{Q} is biased. The expected value of \hat{Q} is:

$$E(\hat{Q}) = Q(1 + v_f / v_s)$$

Note that when the transects are long and perpendicular to the migration, v_s is much smaller than the cruising speed of the vessel. For example, if the cruising speed is 5 ms⁻¹, and the transect length is 10 times the spacing, then the survey progresses at $v_s = 0.5\text{m s}^{-1}$, a value which could well be comparable with v_f . Harden Jones (1968) suggests that herring are capable of migration speeds up to 0.6m s⁻¹. The swimming capability of fish depends on their size, but adult herring and mackerel can sustain speeds around 1.0m s⁻¹ for long periods (He and Wardle 1988; Lockwood 1989). The bias is greatly reduced if the transects run alternately with and against the migration”.

A rough model can be plotted using the equation suggested by Simmonds and MacLennan (2005), with the suggested bias in the survey on the z axis. The start of the survey, the progress speed is about 1.17 m s⁻¹ in the North - direction, indicating that the bias could be from 0 to 50% with a constant fish migration speed of 0.2 m s⁻¹, well within the swimming capacity of adult herring. Using fishery sonar on distinct schools have been tried for direct measurement of the migration speed on earlier surveys, (Slotte et al, 2015,2016), but in this particular spawning survey, only a small fraction of the herring is moving in distinct schools. The more typical situation is layers, either in the water column, or closer to the bottom, as shown in Figure 1, and a better way to measure the migration speed is to use a Doppler system, as realized in a scientific ADCP.

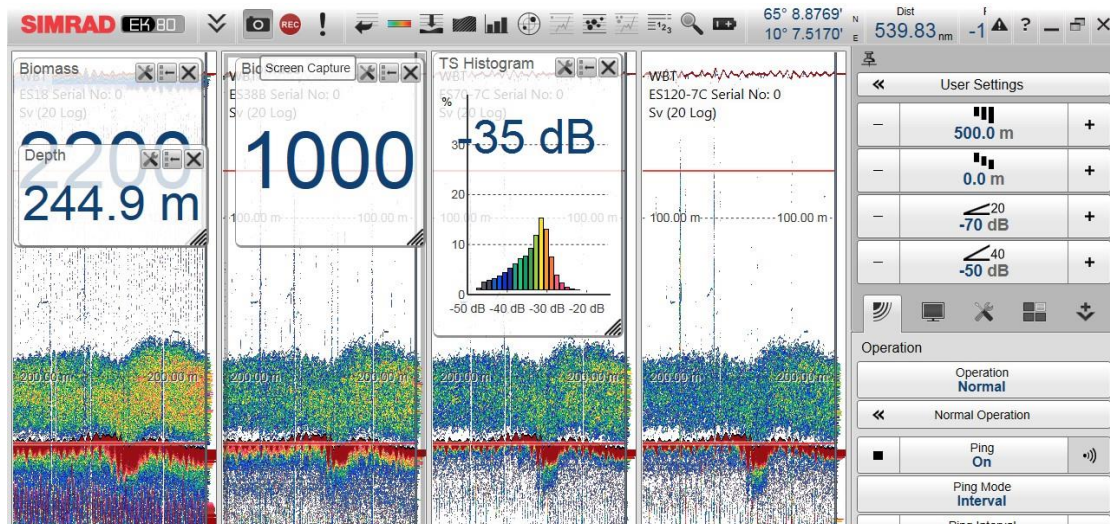
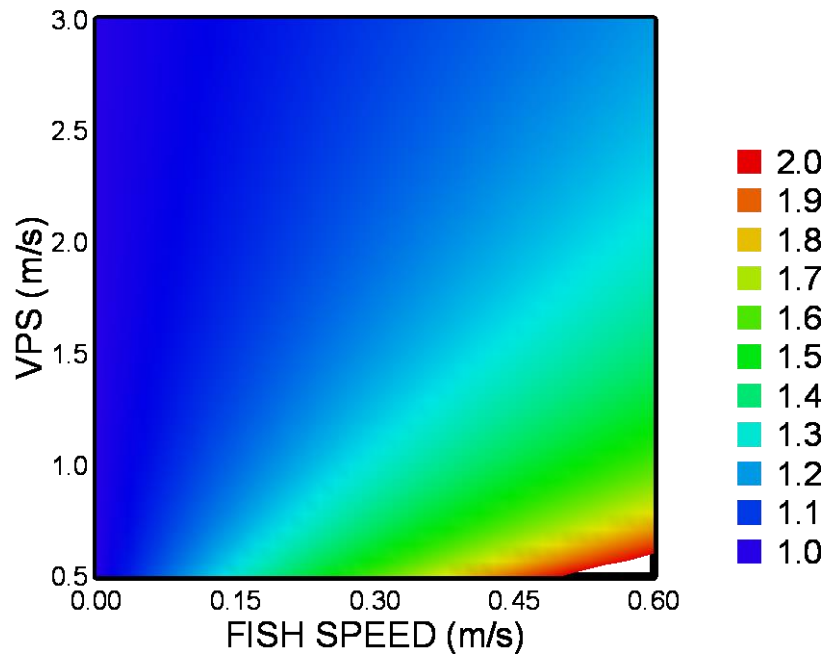


Fig 1. Typical herring layer in the NVG spawning survey (Slotte et al., 2019)



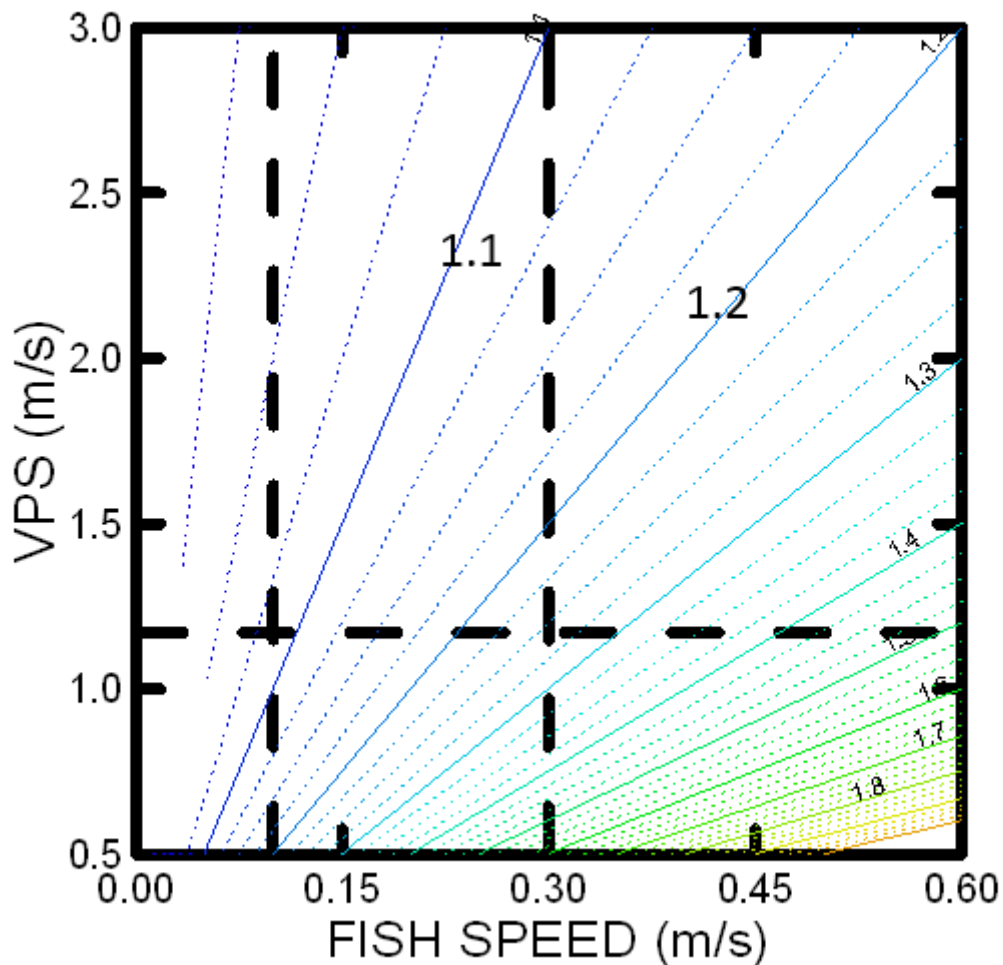


Fig 2. A, B, Overall figures for the migration error as a function of vessel progress speed, VPS (m s⁻¹) and the herring migration speed. Error on Z axis, but with the mean vessel progress speed indicated for all strata 1.17 m s⁻¹ as a vertical line. Observed migration speed for herring is between 0 and 0.3 m s⁻¹, and the potential error can be evaluated to be maximum 1.2, or 20% in the worst case!

Material and methods

A Kongsberg Maritime ES150C EK80 ADCP system, with four acoustic beams transmitting a 150 kHz CW or FM signal installed on MS “EROS” in the dry dock at “Båtbygg”, Måløy, Norway, prior to the survey. The flat array transducer with the EK80 WBT installed in the transducer was transmitting a 12.1 ms CW pulse for the selected settings using phased array steering of the beams in ADCP mode, and a split beam transducer with 3° beam width in broad band echo sounder mode. The system was tested and tried calibrated in Ålesund February 14, 2020. Vessel GPS and KM motion Reference Unit (MRU) were coupled to the instrument, logging raw data to disk on the ADCP system PC.



Fig. 3. ADCP Simrad EC150-3C transducer (and WBT) mounted in box keel in front of the fishery sonars on EROS.

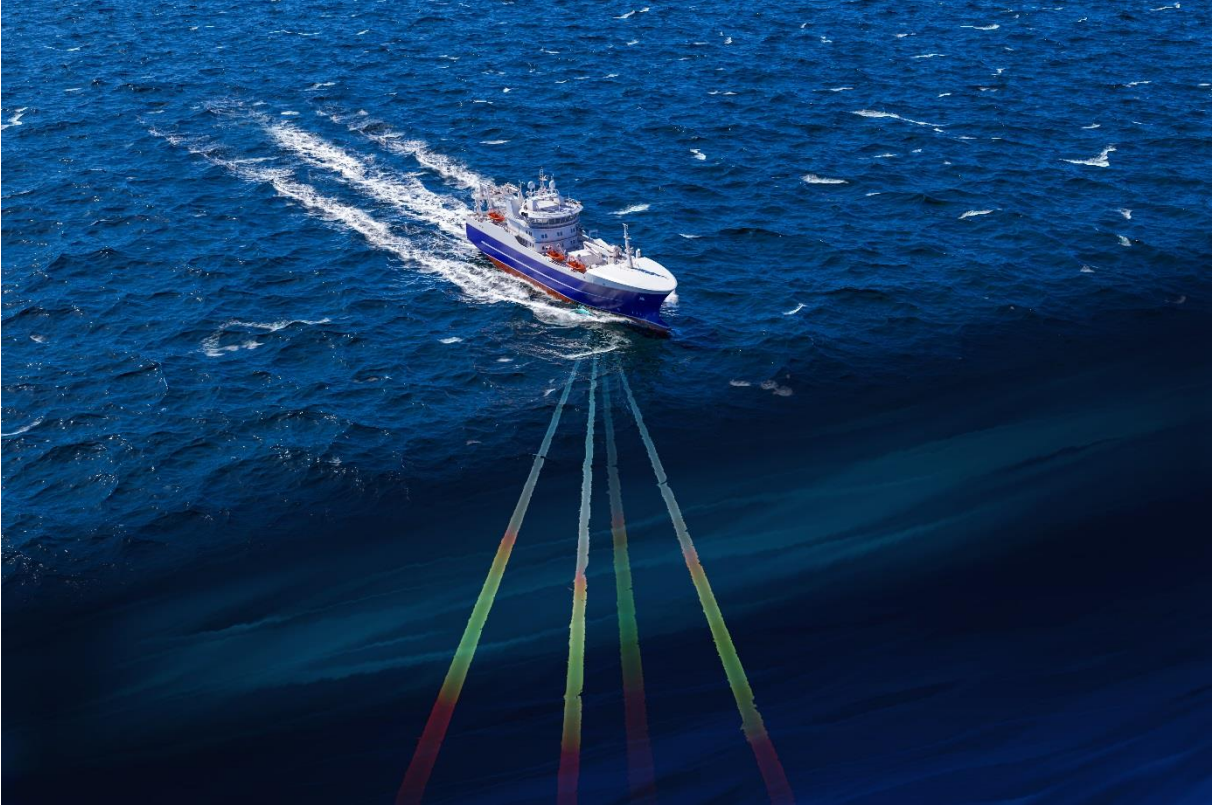


Fig 4. Principal sketch of the Simrad EC150-3C measuring system. (Figure: ©Tonny Algrøy, Kongsberg Maritime)

The ADCP system was run in parallel with the 5 EK60 GPT echo sounders and one SU90 sonar, as a stand-alone system, with no external triggering from the master echo sounder. Only weak interference was observed on the 120 kHz EK60 system, but not enough to disturb the abundance estimation of herring. GPS and a Kongsberg Motion Reference Unit, MRU 5 was connected to the ES150-C system.

The raw data was recorded, and the ADCP generated standard output current profile echograms on the screen, where both the movement of the water current and the herring movement could be monitored in real time.

For stability, averaging over 100 transmissions were used to generate preliminary real time current echograms, but could be re-run in echosounder replay using shorter averaging intervals needed for herring schools. Individual data sets were selected for further inspection and replayed locally on a secondary computer, based upon the scrutinizing results from the survey, using LSSS. During this process, the EK80 generated new processed data files, using standard output in NETCDF format. These were further read by a Python script, where further manipulation of the data could be done. Only preliminary analysis was done during the survey itself.

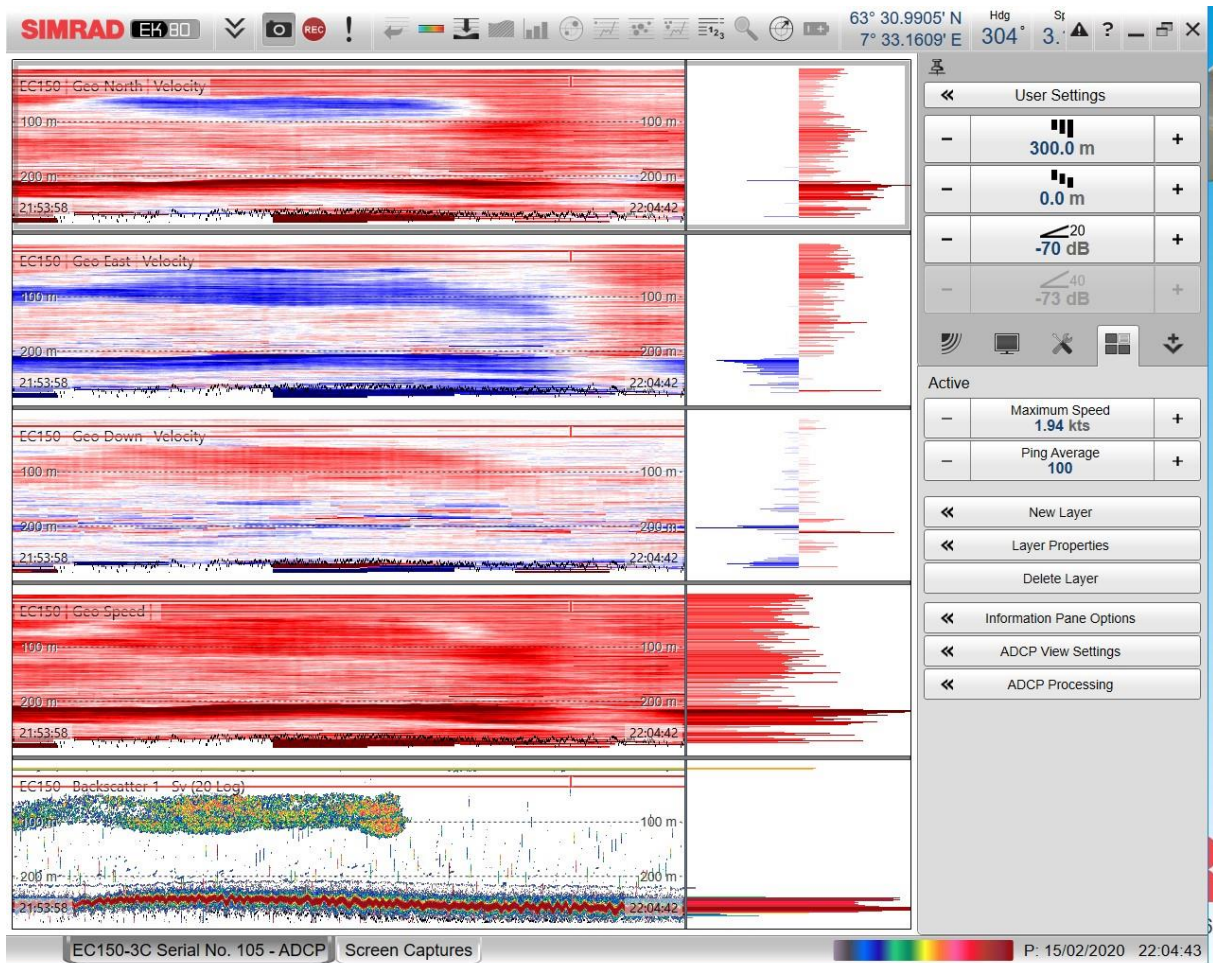


Fig 5. Example display of ADCP processed data. The screen is divided into 4 “echograms” horizontally, where the lower panel shows the backscattering in one of the ADCP beams. The upper panel shows the N/S component, here scaled to 0-2 knots, red is North, blue is South. The panel below the upper one is the E-W display, with similar settings, red is East, blue is West. Then, the third panel is the vertical speed measured, using the same scale, DOWN/ UP, with down as red, up as blue. Further, the last panel shows the sum of the vectors in the previous panels. All measurements here is geo-references, showing movement over ground. It is here clear that the herring swims against the relatively strong coastal current.

Interpretation of example display:

First, the current in this transect is moving in a North direction at about 0.5 knots and slightly towards East. The current speed is similar across the entire whole water column.

The herring, however, is migrating in South direction at 0.5 knots, but also towards East with a similar swimming speed, 0.5 knots, i.e straight against the prevailing current. So, first the herring must compete and overcome the current, and exceeded the water speed with 0.5 knots. Relative to the surrounding water, it is actually swimming at 1 knot, 0.5 m s^{-1} , or about 1.5 bl s^{-1} , which according to Harden Jones (1968) is well within herring migration capacity.

During this first survey, there was no analyzing and processing tools available, and a manual selection of 10 values from the school and 10 values from the water column was selected and stored as separate variables.

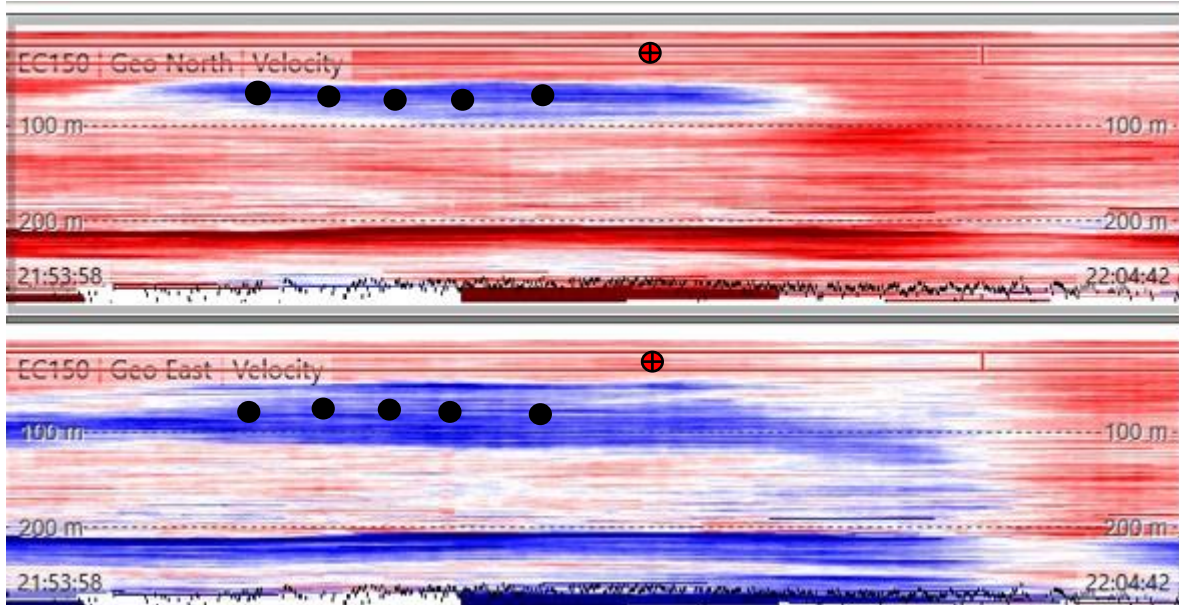


Fig 6. Manual selection of representative swimming speed and current speed, Version 1. In later versions of processing, a mask should be created using LSSS, and the mask transferred to the current echograms. Normal gridding output for both water and herring can then be computed and stored to normal user files.

About 39 data sets have been analyzed during the survey, where the herring swimming speed and current direction have been manually extracted. These data will be used to pair with the density data, either at transect level, or at stratum level.

One could either chose to weigh the speed with the acoustic density, either at transect level or at strata level:

Transect level:

$$h = \frac{\sum_n^i (v_i S_A)}{\sum_n^i S_A}$$

Then, compute the mean backscattered energy weighed speed to be used for the individual strata.

Or at strata level, h could be is the mean speed for all herring inside the strata, and the weight of migration could be the density inside the strata. (not yet decided).

The statistics of the mean survey progress (SPS) speed is shown in the Table 1.

stratum	Δt (H)	S (nmi)	VPS (knots)	VPS (m s ⁻¹)
1	14.39	67.65	4.70	2.42
2	24.64	65.67	2.67	1.37
3	55.74	77.42	1.39	0.71
4	50.55	77.10	1.53	0.78
5	38.02	70.56	1.86	0.95
6	37.32	62.56	1.68	0.86
7	38.45	48.70	1.27	0.65
8	36.66	79.48	2.17	1.12
9	30.21	76.62	2.54	1.30
10	25.53	63.60	2.49	1.28
11	11.01	32.40	2.94	1.51
12	45.78	72.00	1.57	0.81
13	9.01	25.54	2.84	1.46

Table 1. Vessel progress speed in North direction in the different strata of the survey. Delta h is the number of hours inside the strata, and the number of sailed nautical miles inside the strata is S (nmi). Minimum 0.65 m s⁻¹ and maximum 2.41 m s⁻¹ in strata 7 and 1 respectively. The overall mean progress speed is 1.17 m s⁻¹ with a standard deviation of 0.47 m s⁻¹.

We are now working on measuring the mean migration speed for each stratum, but already see that while the migration speed is high in the southern and middle strata, the migration is slower and less systematic further north.

Examples of processed data in Python, after replaying in local EK80 software, and generation of NETCDF output files, is shown below.

If we should make an educated guess at this point, correction for the migration effect on this survey would increase the biomass with 5 to 10%, which is still inside the uncertainty level of the survey estimate.

Egil Ona, At sea 26.2.2020, and home office 30.3.2020.

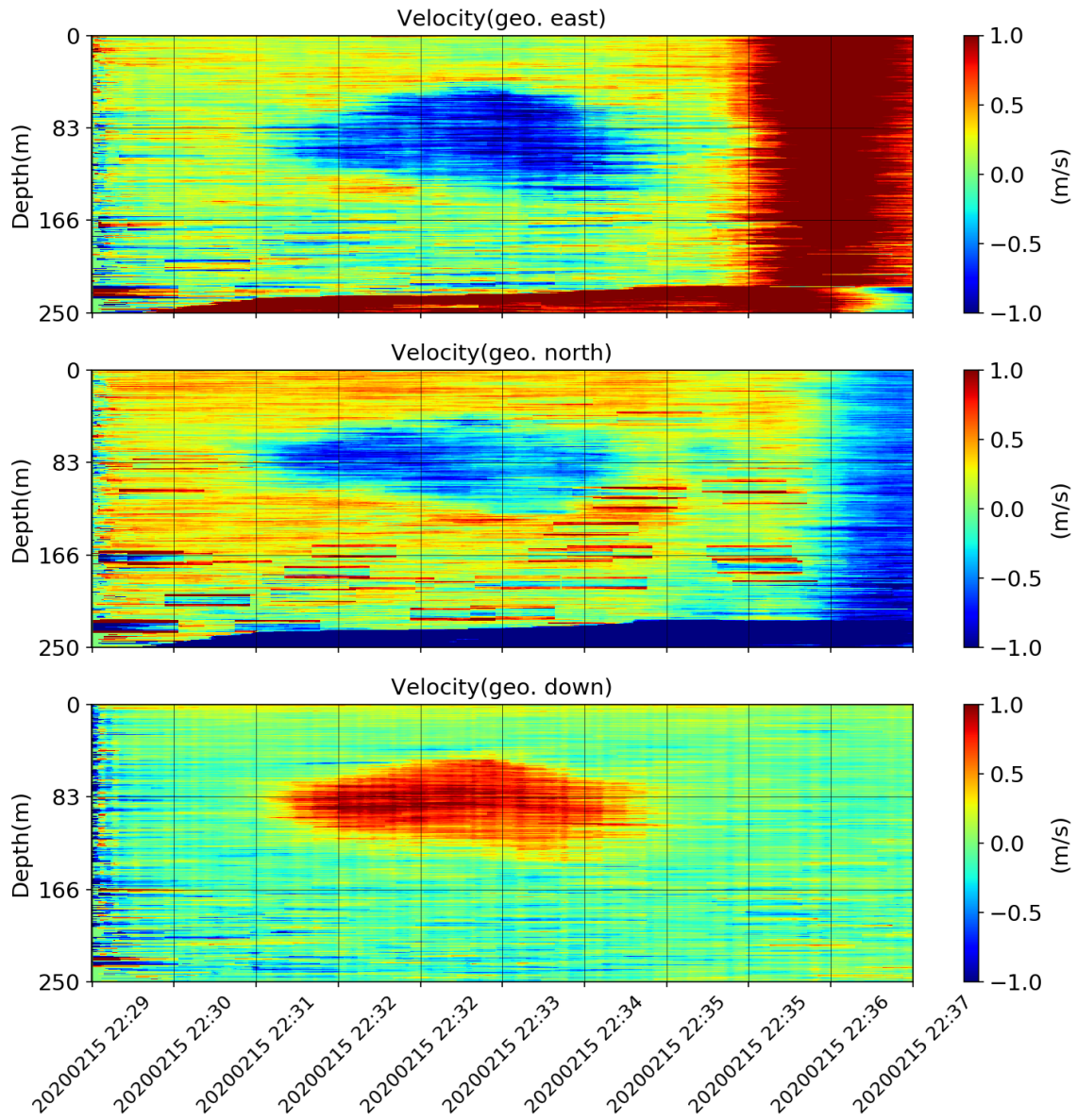


Figure 7. Phyton output of water and herring speed, georeferenced, i.e speed over ground, UPPER (East-West direction, MIDDLE (North-South direction) and LOWER : Vertical direction, Down-Up, with DOWN positive= Red. The dark red in the last part of the “echogram” is connected with a turning of the vessel, a movement which is not compensated for properly, the “sliding movement” of the ship while turning.

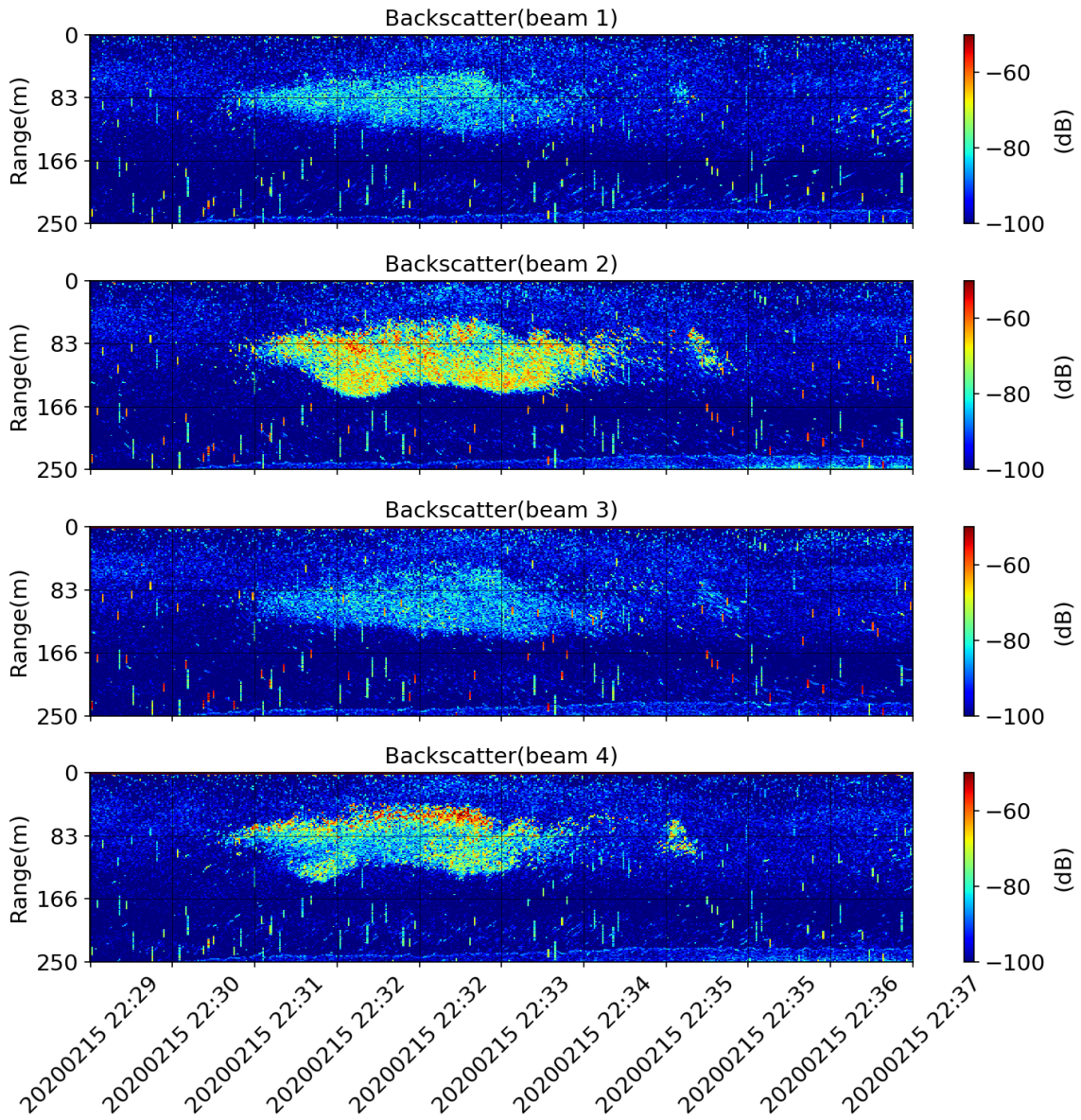


Figure 8. Echogram from the 4 ADCP beams where the Doppler is extracted.